Caporali, A., Meloni, M., Miller, A. M., Vierlinger, K., Cardinali, A., Spinetti, G., Nailor, A., Faglia, E., Losa, S., Gotti, A., Fortunato, O., Mitic, T., Hofner, M., Noehammer, C., Madeddu, P., & Emanueli, C. (2012). Soluble ST2 is regulated by p75 neurotrophin receptor and predicts mortality in diabetic patients with critical limb ischemia. *Arteriosclerosis, Thrombosis, and Vascular Biology*, *32*(12), e149-60. https://doi.org/10.1161/ATVBAHA.112.300497

Peer reviewed version

Link to published version (if available):
10.1161/ATVBAHA.112.300497

Arteriosclerosis, Thrombosis, and Vascular Biology

JOURNAL OF THE AMERICAN HEART ASSOCIATION

Soluble ST2 Is Regulated by p75 Neurotrophin Receptor and Predicts Mortality in Diabetic Patients With Critical Limb Ischemia

Andrea Caporali, Marco Meloni, Ashley M. Miller, Klemens Vierlinger, Alessandro Cardinali, Gaia Spinetti, Audrey Nailor, Ezio Faglia, Sergio Losa, Ambra Gotti, Orazio Fortunato, Tijana Mitic, Manuela Hofner, Christa Noehammer, Paolo Madeddu and Costanza Emanueli

Arterioscler Thromb Vasc Biol. published online October 11, 2012;
Arteriosclerosis, Thrombosis, and Vascular Biology is published by the American Heart Association, 7272 Greenville Avenue, Dallas, TX 75231

Print ISSN: 1079-5642. Online ISSN: 1524-4636

Original Article

Soluble ST2 Is Regulated by p75 Neurotrophin Receptor and Predicts Mortality in Diabetic Patients With Critical Limb Ischemia

Andrea Caporali, Marco Meloni, Ashley M. Miller, Klemens Vierlinger, Alessandro Cardinali, Gaia Spinetti, Audrey Nailor, Ezio Faglia, Sergio Losa, Ambra Gotti, Orazio Fortunato, Tijana Mitic, Manuela Hofner, Christa Noehammer, Paolo Madeddu, Costanza Emanueli

Objective—The p75 neurotrophin receptor ($p75^{NTR}$) contributes to diabetes mellitus–induced defective postischemic neovascularization. The interleukin-33 receptor ST2 is expressed as transmembrane (ST2L) and soluble (sST2) isoforms. Here, we studied the following: (1) the impact of $p75^{NTR}$ in the healing of ischemic and diabetic calf wounds; (2) the link between $p75^{NTR}$ and ST2; and (3) circulating sST2 levels in critical limb ischemia (CLI) patients.

Methods and Results—Diabetes mellitus was induced in *$p75^{NTR}$* knockout (*p75KO*) mice and wild-type (*WT*) littermates by streptozotocin. Diabetic and nondiabetic *p75KO* and *WT* mice received left limb ischemia induction and a full-thickness wound on the ipsilateral calf. Diabetes mellitus impaired wound closure and angiogenesis and increased ST2 expression in *WT*, but not in *p75KO* wounds. In cultured endothelial cells, $p75^{NTR}$ promoted ST2 (both isoforms) expression through $p38^{MAPK}$/activating transcription factor 2 pathway activation. Next, sST2 was measured in the serum of patients with CLI undergoing either revascularization or limb amputation and in the 2 nondiabetic groups (with CLI or nonischemic individuals). Serum sST2 increased in diabetic patients with CLI and was directly associated with higher mortality at 1 year from revascularization.

Conclusion—$p75^{NTR}$ inhibits the healing of ischemic lower limb wounds in diabetes mellitus and promotes ST2 expression. Circulating sST2 predicts mortality in diabetic CLI patients. **(*Arterioscler Thromb Vasc Biol*. 2012;32:00-00.)**

Key Words: diabetes mellitus ■ limb ischemia ■ p75 neurotrophin receptor ■ ST2 ■ wound healing

Critical limb ischemia (CLI) is the end stage of lower extremity peripheral artery disease, in which severe obstruction of blood flow (BF) results in rest pain, ischemic ulcers, and a significant risk for limb loss. Diabetes mellitus (DM) heavily contributes to the prevalence and severity of ischemic disease, through acceleration of atherosclerosisand induction of microangiopathy.[1] Moreover, DM compromises the native neovascularization response, which helps restoring tissue perfusion after an ischemic event.[2,3] The reasons for this angiogenic default in DM are not completely understood. Current revascularization treatments are expensive and mostly palliative, leaving the patient with sequelae and disabilities requiring additional intervention and hospitalization.[4]

The neurotrophin receptor p75 neurotrophin receptor ($p75^{NTR}$) is a member of the tumor necrosis factor (TNF)-α receptors family. We previously demonstrated that $p75^{NTR}$ is implicated in DM-induced impairment of reparative neovascularization[5]. In fact, DM induces $p75^{NTR}$ expression in microvascular endothelial cells (ECs) of ischemic limb muscles and intra-scapular wounds.[6,7] In turn, $p75^{NTR}$ reduces EC survival and functional capacities allowing for the angiogenesis process.[5] The expression and possible pathogenic role of $p75^{NTR}$ in ischemic lower limb ulcers associated or not with DM has never been studied.

The ST2 receptor (also known as interleukin 1 receptor-like 1 [IL1RL1]) belongs to the Toll-like/IL-1–receptor superfamily.[8] Soluble (sST2) and transmembrane (ST2L) isoforms are transcribed from a dual promoter system driving differential mRNA expression.[9] IL-33 belongs to the IL-1 cytokine superfamily and binds both ST2L and sST2. IL-33/ST2L binding leads to activation of transcription factors such as nuclear factor κ-light-chain-enhancer of activated B cells and activator protein 1 via TNF receptor–associated factor-6, IRAK-1/4, and mitogen-activated protein kinases.[10] By contrast, sST2 functions as a decoy receptor.[11] Recent studies

Received on: February 17, 2012; final version accepted on: September, 28, 2012.

From the Laboratories of Vascular Pathology and Regeneration (A. Caporali, M.M., A.N., T.M., C.E.), Experimental Cardiovascular Medicine (P.M.), and Clinical Trial Unit (A. Cardinali), School of Clinical Sciences, University of Bristol, Bristol, England, United Kingdom; Institute of Infection, Immunity and Inflammation, University of Glasgow, Glasgow, Scotland, United Kingdom (A.M.M.); AIT-Austrian Institute of Technology, Vienna, Austria (K.V.,M.H., C.N.); and IRCCS-MultiMedica, Milan, Italy (K.V., M.P.H.).

The online-only Data Supplement is available with this article at http://atvb.ahajournals.org/lookup/suppl/doi:10.1161/ATVBAHA.112.300497/-/DC1.

Correspondence to Costanza Emanueli, PhD, FAHA, Chair of Vascular Pathology and Regeneration, School of Clinical Medicine, Regenerative Medicine Section, University of Bristol, Bristol, BS2 8HW, England, United Kingdom. E-mail c.emanueli@yahoo.co.uk

suggest cardiovascular functions of the IL-33/ST2 system.[12] In particular, IL-33, via ST2L, prevents cardiomyocyte apoptosis and improves cardiac function and survival in mice after myocardial infarct (MI).[13] Moreover, IL-33 promotes angiogenesis[14] and prevents atherosclerosis development.[15] Cellular sources of sST2 in the cardiovascular system include ECs[16,17] and cardiomyocytes.[18] Importantly, sST2 was identified as a novel circulating biomarker of heart failure and MI.[19,20] Moreover, sST2 was proposed to predict mortality in a series of both cardiovascular and noncardiovascular pathological conditions in human patients, including acute MI[21] and heart failure.[22] However, to the best of our knowledge, the IL-33/ST2 system was never investigated in the context of limb ischemia and DM ischemic complications.

Here, taking occasion of our recently established mouse model of ischemic lower limb wound healing[23] and of mice with *p75*^{NTR} gene knockout[24] (*p75KO*), we have studied the impact of *p75*^{NTR} in this experimental setting, associated or not with DM. We provide evidence that *p75*^{NTR} deletion prevents features of delayed wound healing typical of DM, including impaired angiogenesis in the granulation tissue and increased EC apoptosis. Additionally, we have identified that p75^{NTR} positively regulates ST2 expression in both skin wounds and cultured ECs and the molecular pathway that link p75^{NTR} and ST2 in ECs. Moreover, we provide the first ever evidence that circulating sST2 is increased in patients with CLI and DM, where sST2 levels directly correlate with the severity of disease. Finally, we report that in patients with DM and CLI undergoing revascularization to attempt limb salvage, circulating sST2 levels are directly associated with mortality within 1 year of follow-up.

Materials and Methods

Detailed Materials and Methods and human patient characteristics are available in the online-only Data Supplement.

Human Samples

Our study was performed using blood samples of the following: (1) nonischemic, nondiabetic subjects (n=11); (2) nondiabetic CLI patients undergoing revascularization (n=8); (3) diabetic CLI patients undergoing revascularization (n=53); and (4) diabetic CLI patients undergoing limb amputation (n=14). We additionally used samples from limb amputation for immunohistochemical analyses. Patient characteristics are reported in the Table. Clinical outcome at 1 year follow-up was available for the 53 diabetic CLI patients undergoing revascularization, and it is reported in Table I in the online-only Data Supplement. Human studies complied with the ethical principles stated in the Declaration of Helsinki and were covered by ethical approvals for sample and anonymized data collection (IRCCS-Multimedica numbers 020/2008 and 011/2009) and for importing, storage, and analyses of samples at the University of Bristol (NHS-NRES 11SW/0093).

Animal Procedures

All procedures complied with the standards stated in the *Guide for the Care and Use of Laboratory Animals* (Institute of Laboratory Animal Resources, National Academy of Sciences, Washington, DC; 1996) and were approved by the UK Home Office. *WT* littermates and 6- to 7-week-old male *p75KO*[24] (genetic background, C57BL/6J) were made diabetic using streptozotocin[25] or left normoglycemic after STZ buffer. At either 1 or 3 months of diabetes mellitus, left hindlimb ischemia was induced by femoral artery occlusion.[26] At the same occasion, a full-thickness wound was created in the thigh dorsal skin of the ischemic legs using a sterile 5-mm-wide biopsy punch.[23] Laser Doppler was performed at baseline to confirm limb ischemia and at 3, 7, and 14 days thereafter to monitor BF recovery[5,26] Wound closure was analyzed at the same time points.[23]

Table. Clinical Characteristic of Diabetic and Nondiabetic Patients

Patients	No Diabetic Patients, No Ischemic Patients Undergoing Vena Saphena Stripping as Cosmetic Procedure (n=11)	No Diabetic Patients With CLI Undergoing Revascularization (n=8)	Diabetics Patients With CLI Undergoing Revascularization (n=53)	Diabetic Patients With CLI Undergoing Limb Amputation (n=14)
Age, y	61.9±9.1	74.63±9.21	68.46±10.074	68.09±9.06
Sex	5/11 M	5/8 M	38/53 M	10/14 M
Diabetes mellitus	0	0	53/53 TD2	6/14 TD18/14 TD2
HbA1c, % Hb	NR	NR	7.76±1.97	8.08±1.63
Platelet, 10^3/mm	231±69.60	266.37±98.24	291.60±117.67	335.66±104.42
Insulin therapy	0/11 INS	0/8 INS	40/53INS	10/14 INS
Antiplateletdrugs	0	7/8 ASA	37/53 ASA7/53 CLO	2/14 ASA3/14 TICL3/14CLO
		4/8 TICL	16/53 TICL	3/14 TICL
		2/8 CLO	7/53 CLO	3/14CLO
		1/8 AntiCOA	10/53 AntiCOA	0/14 AntiCOA
Antiglycemic drugs	0/11 AGD	0/8 AGD	11/53 AGD	0/14 AGD
Diet	0/11 DI	0/8 DI	2/53 DI	0/14 DI
Hypertension	0/11 HYP	4/8 HYP	35/53 HYP	5/14 HYP
Neuropathy	NR	NR	5/53 NEU	2/14 NEU
Retinopathy	NR	NR	9/53 RET	5/14 RET
CAD	0/11 CAD	3/8 CAD	28/53 CAD	8/14 CAD

TD1 indicates type 1 diabetes mellitus; TD2, type 2 diabetes mellitus; INS, insulin; AGD, antiglycemic drugs; DI, diet; HYP, hypertension; NEU, neuropathy; RET, retinopathy; CAD, coronary artery disease; NR, not recorded; ASA, acetylsalicylic acid; TICL, ticlopidine; CLO, clopidogrel; AntiCOA, dicumarolic anticoagulants.

Immunhistochemistry on Murine and Human Tissues

Histology sections were prepared from mouse ischemic wounds and limb muscles (adductor and gastrocnemious) and from the skin of the amputated lower legs of diabetic CLI patients. In murine sections, capillary and arteriole densities were measured after staining with an antibody for α-smooth muscle actin and for either CD31 or fluorescent isolectin-B4 (EC markers). EC apoptosis was assessed by in situ terminal deoxynucleotidyl transferase dUTP nick end labeling assay combined with CD31 staining. Mouse sections were additionally stained with antibodies for ST2 and $p75^{NTR}$. Human samples were stained for ST2 and IL-33.

RNA Extraction, Microarray, and Quantitative RT-PCR on Mouse Samples

RNA extractions and microarray methods are reported in supplements (GEO accession number, GSE34675). Quantitative RT-PCR for *sfrp1* (secreted frizzled-related protein 1), *Hpx* (hemopexin), *clu* (clusterin), *tnc* (tenascin), *krt20* (keratin 20), *vegfa* (vascular endothelial growth factor A), *vezf1* (vascular endothelial zinc finger 1), *itgb1* (integrin β-1), *birc5* (survivin), *pttg1* (securin), and *il-33* and for the housekeeping *hprt1* (hypoxanthine phosphoribosyltransferase 1) and *rpl13a* (60S ribosomal protein L13a) or *18s* (18s ribosomal RNA) was performed using validated primers (Applied Biosystems). Primers for murine *il1rl1* (*ST2*) enabling to distinguish mRNA expression of sST2 and ST2L isoforms are reported in supplements.

Cells and Cell Culture

Human umbilical vein ECs (HUVECs, Lonza) were grown in EGM-2 (EBM basal medium supplemented with growth factors; Lonza) with 2% fetal bovine serum. When required, HUVECs were cultured in EBM overnight and then stimulated with TNF-α (10 ng/mL R&D Systems), phorbol-12-myristate-13-acetateate (1 μmol/L, Sigma), or vehicles for 16 hours. Small interfering RNA oligonucleotides for $p75^{NTR}$, activating transcription factor 2 (ATF-2) and c-Jun (100 pmol, Dharmacon) or a scrambled oligonucleotide were transfected into HUVECs using Lipofectamine 2000 (Life Technology). Adenoviral vectors carrying human $p75^{NTR}$ or *Null* control are described in Caporali et al[5] and were used as given in Caporali et al.[5]

Western Blot Analyses

Western blot analyses for $p75^{NTR}$, ST2, IL-33, phospo (Thr180/Tyr182), and total p38 mitogen-activated protein kinase ($p38^{MAPK}$), phospho (Thr69/Thr71), and total ATF-2, phospho (Thr183/Tyr185) and total c-Jun N-terminal kinase (Cell Signaling), c-Jun and α/β-tubulin, were performed in HUVECs as described.[5]

ELISA

Concentrations of sST2, VEGF-A, placental growth factor, soluble Tie-2 (sTie-2; angiopoietin-1 receptor), thrombospondin-1 (all from R&D Systems), TNF-α (eBiosciencies), and IL-33 (Prepotech) in HUVEC medium or human serum were quantified by commercial ELISA kits.

Statistical Analyses

Group differences of continuous variables were compared by 1-way ANOVA or Student *t* test, as appropriate. Continuous data are expressed as mean±SEM. A *P* value <0.05 was considered statistically significant. Determinants of the prognostic value of circulating sST2 levels were assessed using multivariate linear regression methods, with the natural log-transformed form of sST2 as the dependent variable. The effect of each determinant was derived from exponentiated regression coefficients.[27] Statistical analyses on patients were completed using R 2.13.3, including the MASS library.

Results

$p75^{NTR}$ Impairs Postischemic Angiogenesis, BF Recovery, and Closure of Ischemic Wounds in Diabetic Mice

When limb ischemia and calf wounds were induced at 1 month of DM, no differences among either *p75KO* and *WT* mice or DM and non-DM were observed in postischemic foot BF recovery or in wound closure (Figure IA and IB in the online-only Data Supplement), which may depend on a longer time required for DM to induce vascular liabilities in c57BL/6J mice. In line with this hypothesis, after 3 months of DM, in *WT* mice, the foot BF recovery was impaired in comparison with age-matched nondiabetic controls ($P<0.05$; Figure 1A). Importantly, *p75KO* mice were protected from DM-induced depressed BF recovery. Moreover, at 14 days postischemia capillary and small arteriole (≤50 μm in diameter) densities in adductor (Figure 1B and 1D) and gastrocnemious (Figure 1C and 1E) muscles were lower in diabetic *WT* mice ($P<0.05$ for all comparisons versus nondiabetic *WT* mice). Noteworthy, capillary and arteriolar densities were normal in diabetic *p75KO* mice (P=NS for all comparisons versus both nondiabetic *WT* mice and nondiabetic *p75KO* mice). As shown in Figure 2A and 2B, in the absence of DM, the ischemic wounds closed similarly in both *p75KO* and *WT* mice. DM compromised the initial phase (3 days) of wound healing in *WT* mice, which confirms what we previously published using an interscapular wound healing model.[23] By contrast, *p75KO* mice were protected from DM-induced impairment of wound closure ($P<0.05$ versus diabetic *WT* mice). Granulation tissue is a vascularized connective tissue that typically grows from the base of a wound to fill it. One of the critical factors for a successful wound healing is the rapid establishment of a perfused granulation tissue.[28] DM in combination with ischemia reportedly impairs the development and maturation of the granulation tissue.[29] Here, we assayed the granulation tissue of 3-day wounds for thickness, vascularity, and EC apoptosis. The granulation tissue thickness was similar in nondiabetic *WT* and *p75KO* and *WT* mice (500±30 μm versus 482±40; P=0.562). In *WT* mice, granulation tissue thickness was reduced by DM (162±13 μm; $P<0.01$ versus non-DM), which simultaneously compromised wound reepithelization. *$p75^{NTR}$* knockout partially preserves skin granulation tissue integrity in diabetic mice. In fact, the *p75KO* diabetic wounds showed a thicker granulation tissue (247±25 μm; $P<0.001$ versus DM in *WT*) and were completely epithelized. Moreover, as shown in Figure 2C, DM reduced wound vascular density in *WT* mice ($P<0.05$ versus non-DM), whereas *p75KO* mice were protected (P=NS and $P<0.05$ versus nondiabetic *WT* and diabetic *WT* mice, respectively). Furthermore, as shown in Figure 2D, DM increased EC apoptosis in ischemic wounds of *WT* mice ($P<0.05$ versus DM) but not in *p75KO* mice (P=NS versus both nondiabetic *WT* and *p75KO* mice and $P<0.05$ versus diabetic *WT* mice).

Taken together, the above data suggest that $p75^{NTR}$ contributes in the delayed healing of ischemic wounds of diabetic

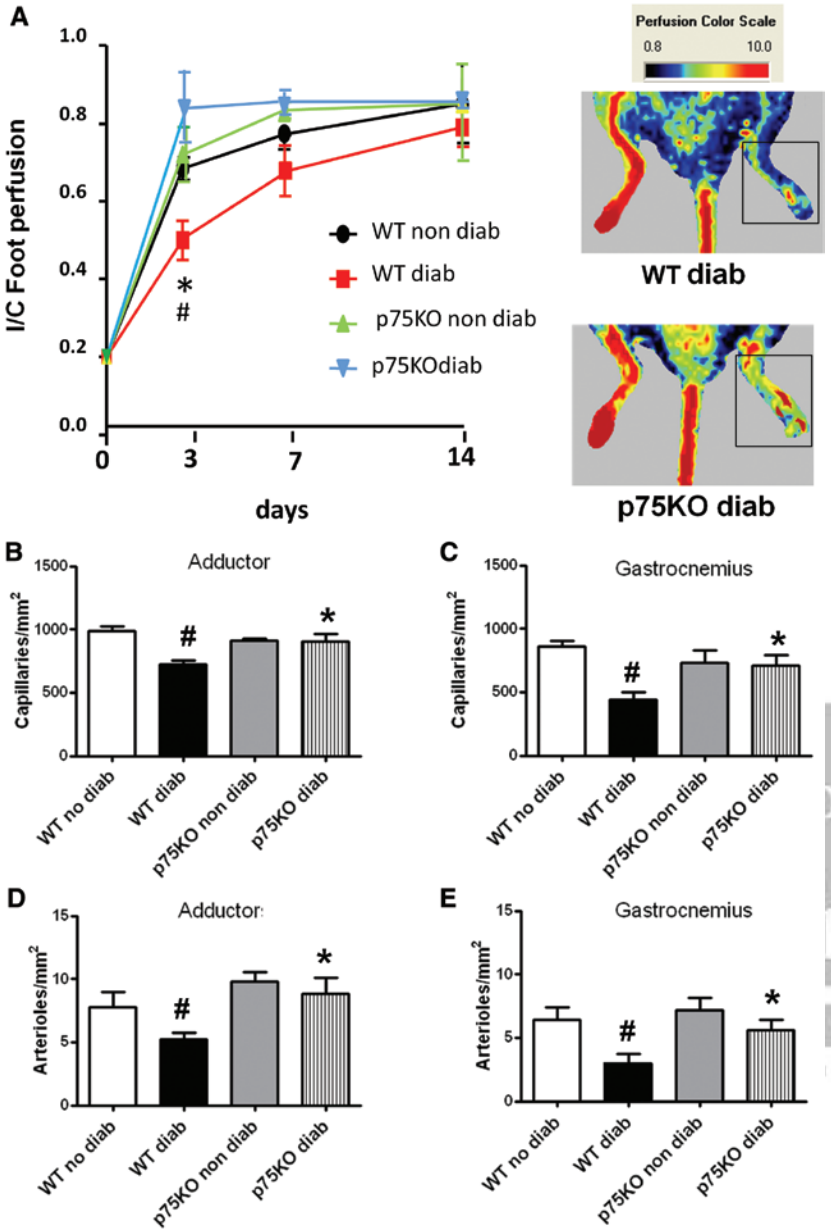

Figure 1. p75 neurotrophin receptor ($p75^{NTR}$) knockout normalizes postischemic neovascularization and blood flow recovery in 3-month diabetic mice. **A**, Unilateral limb ischemia was performed in 3-month diabetic (Diab) and nondiabetic (non diab) wild-type (*WT*) and *p75KO* mice. Representative color laser Doppler images of limb blood flow (BF) taken at 3 days postischemia are shown. Line graph shows the time course of postischemic foot BF recovery (calculated as the ratio between ischemic and contralater foot BF; n=12 mice per group). **B** and **C**, Column graphs show capillary density in ischemic (14 days postsurgery) adductor (**B**) and gastrocnemious (**C**) muscles (n=6 per group). **D** and **E**, Column graphs show small arterioles (diameter <50 mm) densities in ischemic adductors (**D**) and gastrocnemous (**E**) muscles (n=6 per group). **P*<0.05 vs diabetic *WT* mice; #*P*<0.05 vs nondiabetic *WT* mice. Data represent mean±SEM.

mice by impairing the development of the granulation tissue, reducing wound angiogenesis and increasing EC apoptosis.

Effects of Diabetes Mellitus and $p75^{NTR}$ on the Mouse Transcriptomic Profile in Ischemic Skin Wounds and Adductor Muscles

We have previously identified a set of angiogenesis-related genes (*VEGF-A*, *ITGB1*, *VEZF1*, *BIRC5,* and *PTTG1*), which are repressed by $p75^{NTR}$ overexpression in HUVECs.[5] In adductor muscles of *WT* mice, DM decreased the VEGF-A, BIRC5, and PTTG1 mRNA levels, which conversely were elevated in *p75KO* muscles (Figure II in the online-only Data Supplement). In skin wounds of *WT* mice, DM downregulated the mRNA expression of VEGF-A, BIRC5, and VEZF1, whereas *p75KO* diabetic mice maintained a normal (similar to nondiabetic *WT* mice) expression for these genes (Figure III in the online-only Data Supplement).

Next, to identify the whole profile molecular changes associated with the differential responses to DM by *p75KO* mice, parts of the wounds harvested at 3 days were dedicated to mRNA expressional analyses using Agilent 4x44k arrays. Transcriptome analysis (GEO accession number, GSE34675) identified a set of 40 genes differentially expressed in the ischemic wounds of diabetic versus nondiabetic *WT* mice and whose expression in DM was normalized by $p75^{NTR}$ knockout (Table II in the online-only Data Supplement and Figure IVA in the online-only Data Supplement). These genes were clustered for their functional annotation using GeneCodis 2.0[30] (Figure IVB in the online-only Data Supplement). This analysis identified that cytokine–cytokine receptor interaction pathway, cell adhesion molecules, tight junction genes, and leukocyte–EC interaction pathways were mainly affected by DM and $p75^{NTR}$. Among the genes identified accordingly to the

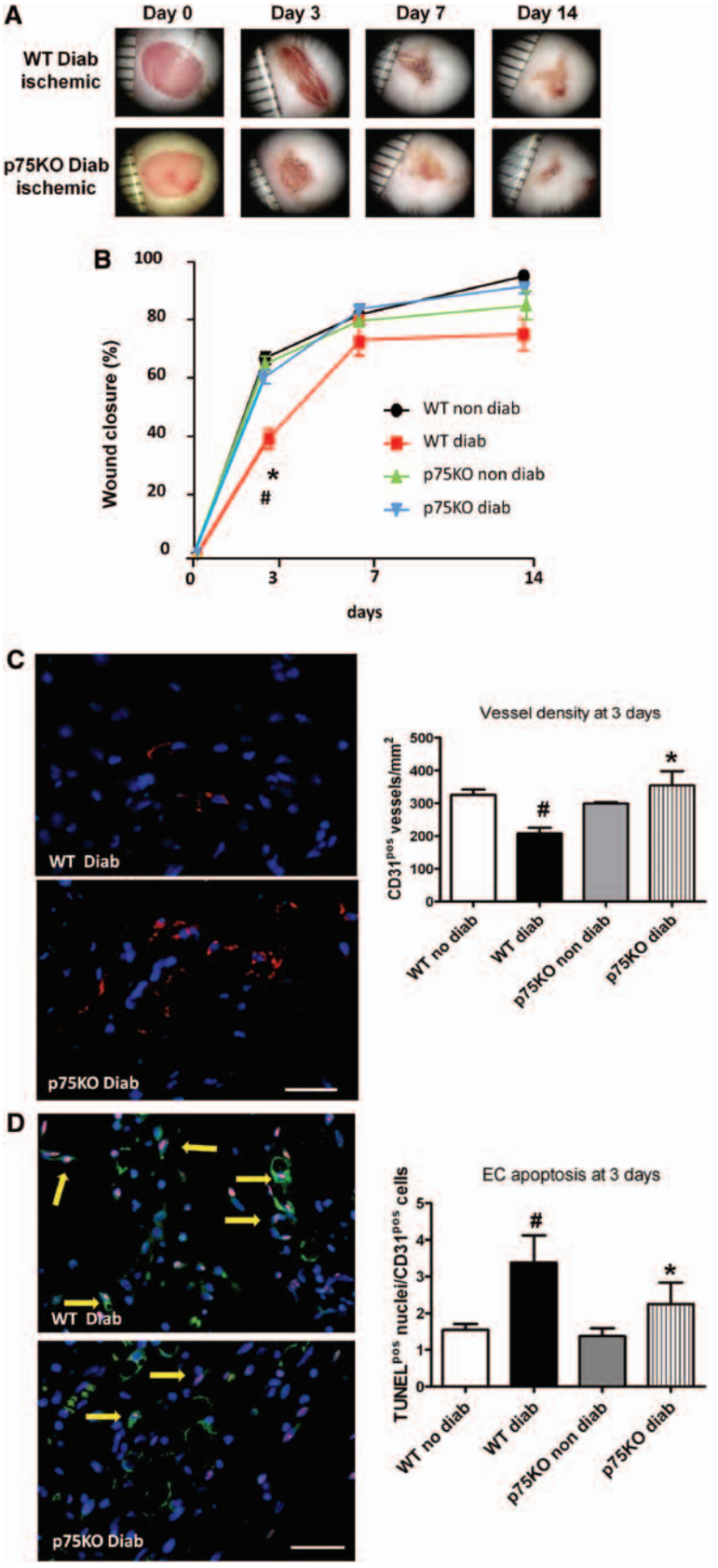

Figure 2. Accelerated wound closure in diabetic *p75KO* mice. **A**, Healing of a 5-mm-diameter cutaneous wound was monitored using digital photography in diabetic (Diab) and nondiabetic (non diab) wild-type (*WT*) and *p75KO* mice with limb ischemia. Representative photos are shown. **B**, Wound size is reported as percentage of the initial wound area. **P*<0.05 vs diabetic *WT* mice; #*P*<0.05 vs nondiabetic *WT* mice. Data represent mean±SEM (n=12). **C**, Capillary density in the granulation tissue was quantified after CD31 staining (red fluorescence). **D**, Apoptosis in endothelial cells (ECs) in granulation tissue was evaluated by costaining with terminal deoxynucleotidyl transferase dUTP nick end labeling (pink merging fluorescence) and CD31 (green fluorescence). Nuclei were counterstained with 4',6-diamidino-2-phenylindole (blue fluorescence). **Arrows** indicate TUNEL-positive EC nuclei. Magnification, ×40. Scale bar, 100 μm **P*<0.05 vs diabetic *WT* mice; #*P*<0.05 vs nondiabetic *WT* mice. Data represent mean±SEM (n=6). KO indicates knockout.

aforementioned defined criteria, 6 genes (*il-1rl1/st2*, *sfrp1*, *clu*, *hpc*, *tnc*, and *Krt20*) were further investigated by quantitative RT-PCR (Figure IVC in the online-only Data Supplement). Next, we decided to focus on ST2 because this receptor is known to be expressed by ECs[16] and involved in angiogenesis[14] and cardiovascular disease.[12] The *ST2* gene produces different sST2 and ST2L mRNA isoforms in both humans and mice.[9] As shown in Figure 3A, both sST2 and ST2L were upregulated at mRNA level by DM in ischemic wounds of *WT* mice ($P<0.05$ for both comparisons versus non-DM). This DM effect was absent in ischemic wounds of *p75KO* mice (P=NS versus nondiabetic *p75KO* and $P<0.05$ versus diabetic *WT* mice). IL-33 mRNA expression showed an inverted pattern of expression in comparison with ST2. ST2L and IL-33 protein expression followed that of mRNA expression (Figure 3B). For ST2 analyzes, we used a polyclonal antibody that recognize human and mouse ST2L, giving a band of ≈ 63 kDa in the mouse wound samples. This antibody did not recognize sST2 in Western blot of mouse skin samples.

Similarly to *WT* wounds, both sST2 and ST2L mRNA were upregulated by DM in adductors of *WT*, but not *p75KO* mice (Figure VA in the online-only Data Supplement). Moreover, IL-33 mRNA expression in skin was downregulated by DM in *WT* mice, only (Figure VA in the online-only Data Supplement).

Localization of ST2 in Vascular Cells in Mouse Adductor Muscles and Skin Wounds

Ischemic dermal wounds and adductor muscles of diabetic *WT* mice were submitted to immunohistochemical analyses. In mouse adductor muscles, ST2 is expressed in smooth muscle cells of arterioles (positive for α-smooth muscle actin; Figure VB in the online-only Data Supplement), but not in capillary ECs (positive for isolectin-B4, Supplementary Figure VC) and it appears additionally expressed by myocytes (Figure VB and VC in the online-only Data Supplement). In mouse skin wounds, ST2 is expressed by microvascular ECs and colocalizes with $p75^{NTR}$ (Figure 3C). These data allow speculating for a possible expressional regulation of the ST2 by $p75^{NTR}$ in vascular cells.

$p75^{NTR}$ Regulates ST2 Expression in Cultured ECs

It was previously shown that impairment of wound healing in diabetic skin correlates with TNF-α expression[31] and that TNF-α increases the secretion of sST2 from ECs.[32] Moreover, TNF-α was shown to promote $p75^{NTR}$ expression in astrocytes.[33] Phorbol-12-myristate-13-acetateate is known to increase the expression of both ST2 forms in ECs[32] and hence can be used as a positive control. We found that 16 hours incubation with either TNF-α or phorbol-12-myristate-13-acetateate upregulated both $p75^{NTR}$ and ST2 protein levels in HUVECs, whereas IL-33 was downregulated (Figure 4A). In HUVECs, the used ST2 antibody detected 2 different bands at 62 kDa and 50 kDa, which probably identify ST2L and sST2, respectively.[34] Western blot analysis on HUVEC conditioned culture medium confirmed the 50-kDa band as released and hence nonmembrane-bound ST2 form (data not shown). Moreover, sST2 concentration in the HUVEC conditioned culture medium was increased by either TNF-α or phorbol-12-myristate-13-acetateate (Figure 4B). Next, the participation of $p75^{NTR}$ in ST2 upregulation was demonstrated using a RNA silencing approach. HUVECs were transfected with oligos for specifically silencing $p75^{NTR}$ and then treated with TNF-α for 16 hours. $p75^{NTR}$ silencing prevented the TNF-α–induced expression of ST2L and sST2 (Figure 4C). In the same experimental setting, the level of sST2 in the HUVEC conditioned culture medium was reduced by $p75^{NTR}$ silencing (Figure 4D). To determine a possible mechanism of regulation of both ST2 isoforms by $p75^{NTR}$, we first investigated the signaling cascade activated in HUVECs in response to $p75^{NTR}$ overexpression achieved by adenovirus (*Ad*)-mediated human $p75^{NTR}$ transfer. One hallmark in $p75^{NTR}$ signaling in neural cells is the activation of the c-Jun N-terminal kinase pathway.[35] However, we did not observe changes in c-Jun N-terminal kinase phosphorylation (Thr183/Tyr185) in ECs transduced with $p75^{NTR}$ (Figure 4E). By contrast, overexpression of the $p75^{NTR}$ for 24 hours induced the phosphorylation (Thr180/Tyr182) of p38MAPK and ATF-2 (Thr69/71), a p38MAPK target (Figure 4E). Phosphorylation of p38MAPK and ATF-2 have been previously demonstrated important for ATF-2 transcriptional activity.[36] Importantly, the increase of ST2L and sST2 expression after $p75^{NTR}$ overexpression was prevented by ATF-2 silencing (Figure 4F and 4G). Moreover, $p75^{NTR}$ overexpression in HUVECs increased c-Jun protein level, and this response was inhibited by ATF-2 knockdown (Figure 4F). Finally, c-Jun silencing further demonstrated that this transcription factor is also required for $p75^{NTR}$-modulated increase in sST2 and ST2L (Figure 4H and 4G).

Expression of the IL-33/ST2 System in Limb Ulcers and Serum of Patients With CLI and DM

To investigate whether our findings in mice and cultured ECs could have a potential clinical relevance, we examined the expression of $p75^{NTR}$, ST2, and IL-33 in skin samples obtained from major limb amputation of diabetic CLI patients (patients are described in the Table). As shown in Figure VI in the online Data Supplement, $p75^{NTR}$ was expressed in small arteries of the adventitia (red arrow), in venules (yellow arrows), and in microvessels (white arrow). Similarly, ST2 was expressed in venules (yellow arrows) and in microvessels (white arrows). IL-33 localization was predominantly in the nuclei of EC (green arrows) belonging to blood vessels of different calibres, as previously reported for other organs also in nondiabetic subjects.[37]

Next, we measured serum levels of sST2 and IL-33 in 4 group of subjects (see the Table): nondiabetic and nonischemic patients undergoing vena saphena stripping (controls, n=11); nondiabetic patients with CLI undergoing revascularization to attempt limb salvage (n=8); diabetics patients with CLI undergoing revascularization (n=53); and diabetic patients with CLI undergoing major limb amputation (n=14). As shown in Figure 5A, in nondiabetic CLI patients undergoing revascularization, sST2 levels were comparable with controls (153.4±62.6 pg/mL versus 142.8±41.2 pg/mL; P=NS). By contrast, serum sST2 levels were higher

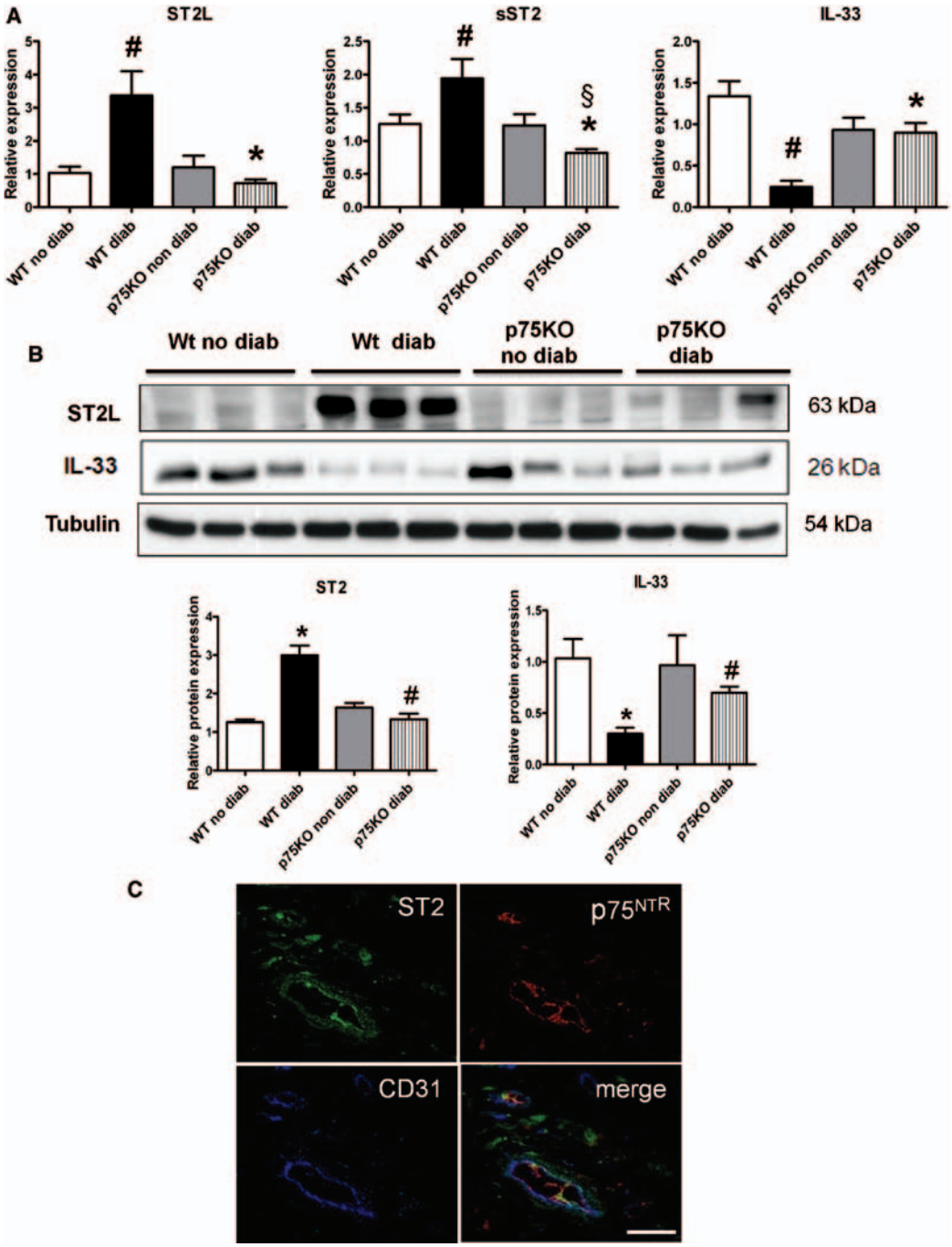

Figure 3. ST2/interleukin-33 (IL-33) characterization in skin wounds. **A**, Relative expression of ST2L, sST2, and IL-33 in skin wounds of diabetic and nondiabetic wild-type (WT) and p75KO mice. Results were normalized to 18S expression. Data represent mean±SEM, n=5. **P*<0.05 vs diabetic WT mice; #*P*<0.05 vs nondiabetic WT mice; §*P*<0.05 vs nondiabetic p75KO mice. **B**, Representative Western blot analyses of ST2L and IL-33 in skin wounds of diabetic and nondiabetic WT and p75KO mice. Bar graphs show relative protein quantification of ST2L and IL-33. Relative values are normalized by α/β Tubulin levels. Western blot data represent means± SD, n=3. **P*<0.05 vs diabetic WT mice; #*P*<0.05 vs nondiabetic WT mice. **C**, Fluorescent immonocytochemistry for ST2 (green fluorescence), p75 neurotrophin receptor (p75NTR; red fluorescence), and CD31 (blue fluorescence) in skin wounds of diabetic WT mice. Magnfication, ×63. Scale bar, 50 μm.

in diabetic CLI patients undergoing revascularization (271.8±138.7 pg/mL; *P*<0.05 versus healthy) and further increased in even more compromised diabetic CLI patients, who necessitated major limb amputation (552.5±118.7 pg/mL; *P*<0.05 versus any other group). We could not detect IL-33 in the serum of our patients and control subjects. As shown in Figure VII in the online-only Data Supplement, circulating level of TNF-α increased in serum of diabetic patients undergoing revascularization, only (37.7±9.3 pg/mL versus 10±4.2 pg/mL in healthy controls; *P*<0.05). Circulating VEGF-A, sTie-2, and thrombospondin-1 levels were found elevated in patients with severe peripheral artery disease and their expression to correlate with the severity of the disease.[38,39] In addition, serum levels of placental growth

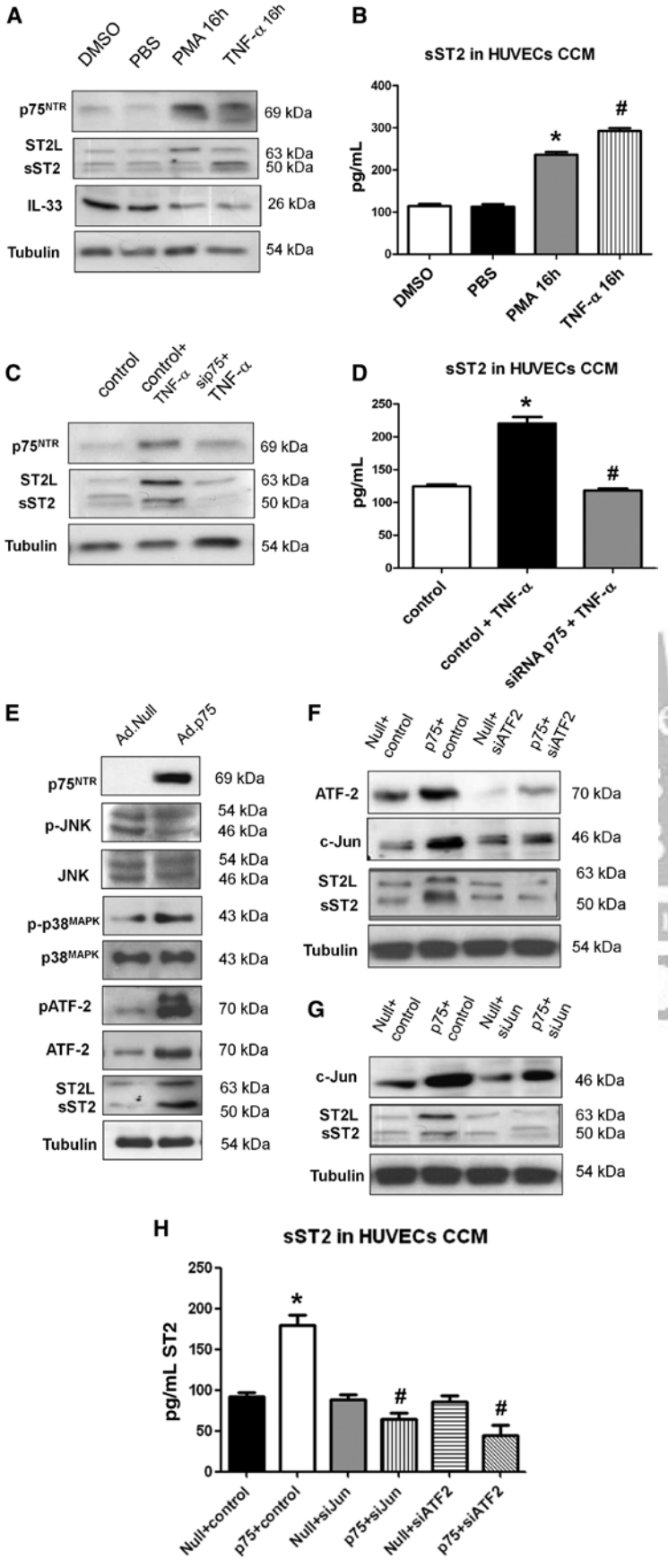

Figure 4. p75 neurotrophin receptor (p75^{NTR}) regulates the expression of ST2. **A**, Representative Western blot bands for p75^{NTR}, ST2, and interleukin (IL)-33 proteins of human umbilical vein endothelial cells (HUVECs) treated with treated for 16 hours with either tumor necrosis factor-α (TNF-α) at the concentration of 10 ng/mL or phorbol-12-myristate-13-acetateate (PMA) at the concentration of 1 μmol/L for 16 hours (data are quantified in Supplementary Figure 9A). **B**, Detection of sST2 by ELISA assay in the medium of HUVECs treated as reported above. *P<0.05 vs dimethyl sulfoxide (DMSO); #P<0.05 vs PBS. **C,** HUVECs were transfected with small interfering RNA (siRNA) oligos for p75^{NTR} or control oligos and treated with TNF-α for 16 hours. Representative Western blot bands for p75^{NTR} and ST2 (data are quantified in Figure IXB in the online-only Data Supplement). **D,** Detection of sST2 by ELISA assay in the medium of HUVECs after p75^{NTR} silencing and TNF-α treatment. ELISA data represent mean±SEM, *P<0.05 vs control; #P<0.05 vs control+TNF-α. (n=3). **E**, Representative Western blot analyses for p75^{NTR}, phospho–c-Jun N-terminal kinase (p-JNK), JNK, phospho–mitogen-activated protein kinase (p-p38^{MAPK}), p38^{MAPK}, phospho–activating transcription factor 2 (p-ATF-2), ATF-2, and ST2 proteins of HUVECs cells infected with adenovirus *(Ad).Null* or *Ad.p75^{NTR}* (data are quantified in Figure XIE in the online-only Data Supplement). **F,** Representative Western blot bands for ATF-2, c-Jun, and ST2 proteins of HUVECs transfected with ATF-2 siRNA oligos and subsequently infected with *Ad.Null* or *Ad.p75^{NTR}* (data are quantified in Figure XIF in the online-only Data Supplement). **G**, Representative Western blot bands for c-Jun and ST2 proteins of HUVECs cells transfected with c-Jun siRNA oligos and subsequently infected with *Ad.Null* or *Ad.p75^{NTR}* (data are quantified in Figure XIG in the online-only Data Supplement). **H**, Detection of sST2 by ELISA assay in the medium of HUVECs after ATF-2, c-Jun silencing, p75^{NTR} or null transduction. ELISA data represent mean±SEM. *P<0.05 vs Ad.Null+control; #P<0.05 vs control+Ad.p75^{NTR} (n=3).

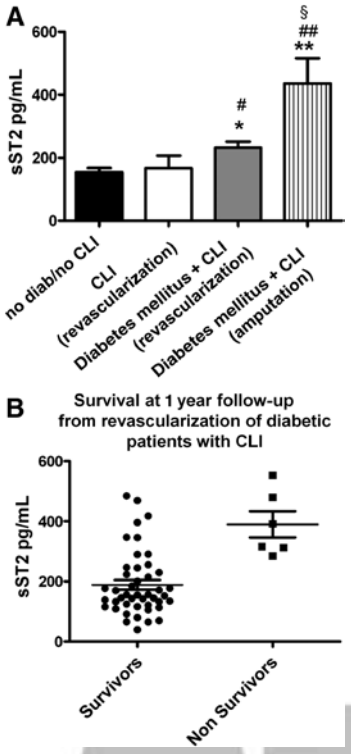

Figure 5. Serum soluble ST2 (sST2) levels in critical limb ischemia patients. **A**, Serum sST2 level in nondiabetic nonischemic patients (controls, n=11), nondiabetic patients with critical limb ischemia (CLI) undergoing revascularization to attempt limb salvage (n=8), diabetic patients with CLI undergoing revascularization (n=53), and diabetic patients with CLI undergoing limb amputation (n=14). ELISA data represent mean±SEM. **P*<0.05 and ***P*<0.01 vs controls; #*P*<0.05 and ##*P*<0.01 vs nondiabetic CLI patients undergoing revascularization; §*P*<0.05 vs diabetic CLI patients undergoing revascularization. **B**, Dot plot shows the baseline concentrations of sST2 in patients experiencing death and the survivor group (at 1-year follow-up).

factor are reportedly elevated in patients with ischemic cardiomyopathy.[40] We measured these 4 factors in our patient populations. As shown in Figure VII in the online-only Data Supplement, VEGF-A, sTie-2, and thrombospondin-1 were similarly elevated in the 3 groups of CLI, whereas placental growth factor was increased in diabetic patients with CLI undergoing major limb amputation only.

Serum sST2 Level Correlates With Mortality in Diabetic CLI Patients Undergoing Revascularization

Next, limited to the 53 diabetic patients undergoing revascularization to treat CLI, we investigated whether circulating sST2 level could be statistically associated with baseline clinical variables (Table) or clinical outcomes (Table I in the online-only Data Supplement) at 1-year follow-up from revascularization. Because of the moderate sample size, in our analysis we avoided the use of nonlinear modeling approaches, such as generalized (GLM) or additive (GAM) regression models, because these typically require a larger amount of data to provide efficient and reliable estimates. We rather used a data transformation in association with a linear regression model. We had evidence of substantial Gaussianization effect, and therefore we adopted the logST2 as response variable in a linear regression model. Most baseline clinical characteristics, including sex, age, DM-related pathologies, hemoglobin A1c level, and extent of coronary artery disease, did not correlate with baseline sST2 level. Furthermore, at least in our data set, there is no evidence for a significant effect of VEGF-A, Tie-2, placental growth factor, and thrombospondin-1 on log ST2. The continuous variable TNF-α has a nonsignificant effect, in agreement with data published by Shimpo et al[21] in acute MI. By contrast and importantly, both indicator variables for antiglycemic medications and for death of patients during 1-year follow-up have a significant effect on sST2 (Table III in the online-only Data Supplement). In particular, the antiglycemic medication had a strong effect in reducing the level of sST2 (Figure VIII in the online-only Data Supplement), whereas the death within 1-year follow-up was directly related to increased levels of sST2 (Figure 5B).

Finally, it has been demonstrated that there is a significant negative correlation between circulating levels of sST2 and platelets counts in dengue-infected patients.[41] We did not find any significant difference in the level of sST2 between plasma and serum in healthy volunteer (plasma, 148±12 pg/mL; serum, 153±22 pg/mL; *P*=0.777; n=5). In our patients, no significant correlation between platelet counts and level of circulating ST2 (*r*=–0.0773; *P*=0.953) and nonsignificant effect on the variable sST2 have been detected (Table III in the online-only Data Supplement). Moreover, indicator variables for antiplatelet drugs (acetyl salicylic acid, clopidogrel, ticlopidine, and dicumarolic anticoagulants) have nonsignificant effect on sST2 (Table III in the online-only Data Supplement).

Taken together, these data provide the first evidence that sST2 measured immediately before revascularization of ischemic limb predicts mortality at 1-year follow-up and that the level of circulating sST2 inversely correlates with the use of antiglycemic medications.

Discussion

Diabetic patients exhibit an insufficient capacity in the healing of acute wounds, which often develop into chronic ulcers in their feet and lower limbs. The impaired wound healing response in diabetic subjects involves multiple and complex pathophysiological mechanisms, including defective angiogenesis. We already provided evidences that DM induces $p75^{NTR}$ expression in ECs of intra-scapular skin wounds[7] and ischemic limb muscles.[6] We also demonstrated that $p75^{NTR}$ impairs EC survival and functions and that its expression is responsible for DM-induced defective postischemic angiogenesis in limb muscles.[5]

Here, we report for the first time that *p75*^{NTR} gene deletion accelerates the healing of ischemic skin wound in the lower limbs of diabetic mice. To better mimic human diabetic ulcers, a full excisional skin wound was created in the calf area of diabetic mice after induction of ipsilateral limb ischemia. In this model, which was recently established by us[23] and already validated by others,[29] the presence of muscular ischemia further delays wound healing. Importantly, when subjected to this model, diabetic *p75KO* mice exhibited accelerate wound closure, improved reparative angiogenesis, and reduced EC apoptosis in granulation tissue in comparisons

with diabetic *WT* mice. Moreover, in diabetic *p75KO* mice, both postischemic muscular angiogenesis and foot BF recovery were better than in diabetic *WT* mice, thus confirming the results that we previous obtained after local *Ad*-mediated transfer of a $p75^{NTR}$ dominant negative mutant form to inhibit receptor activity in diabetic *WT* mice with limb ischemia.[5]

To profile the molecular changes associated with $p75^{NTR}$ and DM in ischemic wounds, we used a RNA microarray. Transcriptome analysis identified a set of genes differentially expressed in diabetic versus nondiabetic *WT* mice and whose expression was normalized by $p75^{NTR}$ knockout. These genes were clustered for their functional annotation, showing enrichment for genes involved in cytokine–receptor interaction pathway, cell adhesion molecules, tight junction genes, and leukocytes transendothelial migration pathways. We noted that components of these pathways were upregulated by DM in the presence of the $p75^{NTR}$ only. We decided to focus on ST2 to further develop our study. ST2 was already known to be expressed by ECs[16] and involved in inflammatory angiogenesis.[14] In skin, ST2 is expressed in ECs and keratinocytes. However, ST2 role in ischemic complication of DM was unknown, as well as the mechanisms of induction of ST2 expression in diabetic wound healing. ST2 expression in ECs is known to be modulated by proinflammatory cytokines, including TNF-α.[32] Moreover, type 2 DM is associated with high serum levels of TNF-α and high local TNF-α levels have been identified as a molecular predictive factor for nonhealing ulcers.[42] In this study, we found circulating TNF-α to be increased in patients with DM and CLI requiring revascularization, but not in diabetic CLI patients requiring amputation. Notwithstanding, TNF-α supplementation proved a good model to induce $p75^{NTR}$ and ST2 expression in cultured ECs and helped define the importance of $p75^{NTR}$ for ST2 expression in ECs. In fact, $p75^{NTR}$ silencing prevented ST2 expression in TNF-α–stimulated ECs. Importantly, in vivo, $p75^{NTR}$ and ST2 colocalize in dermal EC of diabetic murine wounds, which reinforces the possibility of a dependence of ST2 from $p75^{NTR}$. Next, we went more insight the mechanisms mediating ST2 regulation by $p75^{NTR}$. In ECs, the $p38^{MAPK}$ pathway is activated by stress-inducing stimuli, including reactive oxygen species, hyperglycemia, and proinflammatory cytokines, such as TNF-α.[43] Here, we have identified that increased $p75^{NTR}$ levels induce the phosphorylation of $p38^{MAPK}$ and ATF-2 in HUVECs, whereas c-Jun N-terminal kinase pathway is not involved. Moreover, using a gene silencing approach, we have demonstrated that ATF-2 and c-Jun are regulated by $p75^{NTR}$ and are both necessary for ST2 transcription. The ST2 proximal promoter is predominantly responsible for both ST2 isoforms expression in ECs,[16] and it is mainly regulated by activator protein 1 transcription factor complex.[44] Whereas ATF-2 forms homodimers that bind CRE-like recognition sequences, the heterodimers with other activator protein 1 family members, such as c-Jun, allow for binding to typical activator protein 1 sequences in gene promoters.[36] In addition, the ATF-2 direct transcriptional regulation of c-Jun is activated by stress-inducing stimuli in a wide number of cell lines.[45] In response to $p75^{NTR}$ stimulation, cells induce both the upregulation of c-Jun and the activation of ATF-2, which could possibly bind together to ST2 proximal promoter and converge in the activation of its transcription.

sST2 has been recently proposed as a novel diagnostic biomarker for cardiovascular disease, including acute MI and heart failure.[19,20,27,46] Moreover, Sabatine et al showed highly significant increase in circulating sST2 in post-MI patients with DM. We have measured sST2 in the serum of diabetic patients with CLI requiring either revascularization for attempting limb salvage or amputation as only relief from unbearable pain and terminal gangrene. Circulating sST2 levels were higher in diabetic CLI patients undergoing revascularization in comparison with either nondiabetic CLI patients or healthy subjects. Serum sST2 further increased in diabetic patients at the moment of lower limb amputation. Importantly, in our patient cohorts, sST2 was not associated with the extent of coronary artery disease, thus excluding the possibility that our findings in CLI simply reflects the fact that sST2 is biomarker of heart disease.[19,20]

For the 53 diabetic CLI patients undergoing revascularization, the clinical follow-up at 1 year was available, allowing investigation of the value of sST2 as a predictor of clinical outcome. Using a statistical linear regression model, in this patient population, sST2 was directly associated with mortality within 1 year of follow-up.

A handful of studies had previously suggested the capacity of circulating sST2 to predict mortality, both in cardiovascular and noncardiovascular patients.[21,22] The reasons by which sST2 could associate with mortality are still unexplored. A limit of our study is that the cause of death for some of the patients enrolled in our study was not recorded. A prospective study using a larger diabetic CLI patient population is necessary to shed light on the mechanisms underpinning the link of sST2 and death. Moreover, it would be important to understand whether the mechanisms by which sST2 can predict death in diabetic CLI patients are different or similar to those by which sST2 predicts mortality in other cardiovascular and noncardiovascular patient populations.[21] An additional limitation of this study is that it is based on a relatively small sample size (n=53), and it was neither designed nor powered for analysis of effects of sST2 on mortality or its interaction with other variables; therefore, these results should be considered as hypothesis-generating only. We would tend to discard the possibility that increased sST2 further compromises ulcer healing, because in a pilot experiment, we did not record any negative responses to topical application of sST2 on cutaneous ischemic wounds, which closed normally (Meloni, unpublished data, 2011).

In our clinical study, IL-33 could not be detected in the serum of any of the studied groups. Whereas circulating IL-33 is elevated in inflammatory diseases such as rheumatoid arthritis,[47] levels of IL-33 freely circulating in the blood of cardiovascular patients are likely to be low, possibly because of the elevated sST2 levels.

In conclusion, our data identified and describe, for the first time, a link between $p75^{NTR}$ and ST2 and propose sST2 as possible diagnostic and prognostic biomarker in diabetic patients with CLI. Further studies are necessary to validate the biomarker value of sST2.

Sources of Funding

Financial support was provided by a project grant, a senior research fellowship (C. Emanueli), and 2 intermediate research fellowships (AC and A.M. Miller) from the British Heart Foundation and by grants from the European Community (FP7 RESOLVE integrated project) and the Italian Ministry of Health.

Disclosures

None.

References

1. Faglia E. Characteristics of peripheral arterial disease and its relevance to the diabetic population. *Int J Low Extrem Wounds*. 2011;10:152–166.
2. Rivard A, Silver M, Chen D, Kearney M, Magner M, Annex B, Peters K, Isner JM. Rescue of diabetes-related impairment of angiogenesis by intramuscular gene therapy with adeno-VEGF. *Am J Pathol*. 1999;154:355–363.
3. Emanueli C, Caporali A, Krankel N, Cristofaro B, Van Linthout S, Madeddu P. Type-2 diabetic Lepr(db/db) mice show a defective microvascular phenotype under basal conditions and an impaired response to angiogenesis gene therapy in the setting of limb ischemia. *Front Biosci*. 2007;12:2003–2012.
4. Norgren L, Hiatt WR, Dormandy JA, Nehler MR, Harris KA, Fowkes FG, Rutherford RB; TASC II Working Group. Inter-society consensus for the management of peripheral arterial disease. *Int Angiol*. 2007;26:81–157.
5. Caporali A, Pani E, Horrevoets AJ, Kraenkel N, Oikawa A, Sala-Newby GB, Meloni M, Cristofaro B, Graiani G, Leroyer AS, Boulanger CM, Spinetti G, Yoon SO, Madeddu P, Emanueli C. Neurotrophin p75 receptor (p75NTR) promotes endothelial cell apoptosis and inhibits angiogenesis: implications for diabetes-induced impaired neovascularization in ischemic limb muscles. *Circ Res*. 2008;103:e15–e26.
6. Salis MB, Graiani G, Desortes E, Caldwell RB, Madeddu P, Emanueli C. Nerve growth factor supplementation reverses the impairment, induced by Type 1 diabetes, of hindlimb post-ischaemic recovery in mice. *Diabetologia*. 2004;47:1055–1063.
7. Graiani G, Emanueli C, Desortes E, Van Linthout S, Pinna A, Figueroa CD, Manni L, Madeddu P. Nerve growth factor promotes reparative angiogenesis and inhibits endothelial apoptosis in cutaneous wounds of Type 1 diabetic mice. *Diabetologia*. 2004;47;1047–1054.
8. Tominaga S. A putative protein of a growth specific cDNA from BALB/c-3T3 cells is highly similar to the extracellular portion of mouse interleukin 1 receptor. *FEBS Lett*. 1989;258:301–304.
9. Iwahana H, Yanagisawa K, Ito-Kosaka A, Kuroiwa K, Tago K, Komatsu N, Katashima R, Itakura M, Tominaga S. Different promoter usage and multiple transcription initiation sites of the interleukin-1 receptor-related human ST2 gene in UT-7 and TM12 cells. *Eur J Biochem*. 1999;264:397–406.
10. Schmitz J, Owyang A, Oldham E, Song Y, Murphy E, McClanahan TK, Zurawski G, Moshrefi M, Qin J, Li X, Gorman DM, Bazan JF, Kastelein RA. IL-33, an interleukin-1-like cytokine that signals via the IL-1 receptor-related protein ST2 and induces T helper type 2-associated cytokines. *Immunity*. 2005;23:479–490.
11. Sanada S, Hakuno D, Higgins LJ, Schreiter ER, McKenzie AN, Lee RT. IL-33 and ST2 comprise a critical biomechanically induced and cardioprotective signaling system. *J Clin Invest*. 2007;117:1538–1549.
12. Miller AM, Liew FY. The IL-33/ST2 pathway–A new therapeutic target in cardiovascular disease. *Pharmacol Ther*. 2011;131:179–186.
13. Seki K, Sanada S, Kudinova AY, Steinhauser ML, Handa V, Gannon J, Lee RT. Interleukin-33 prevents apoptosis and improves survival after experimental myocardial infarction through ST2 signaling. *Circ Heart Fail*. 2009;2:684–691.
14. Choi YS, Choi HJ, Min JK, Pyun BJ, Maeng YS, Park H, Kim J, Kim YM, Kwon YG. Interleukin-33 induces angiogenesis and vascular permeability through ST2/TRAF6-mediated endothelial nitric oxide production. *Blood*. 2009;114:3117–3126.
15. Miller AM, Xu D, Asquith DL, Denby L, Li Y, Sattar N, Baker AH, McInnes IB, Liew FY. IL-33 reduces the development of atherosclerosis. *J Exp Med*. 2008;205:339–346.
16. Aoki S, Hayakawa M, Ozaki H, Takezako N, Obata H, Ibaraki N, Tsuru T, Tominaga S, Yanagisawa K. ST2 gene expression is proliferation-dependent and its ligand, IL-33, induces inflammatory reaction in endothelial cells. *Mol Cell Biochem*. 2010;335:75–81.
17. Bartunek J, Delrue L, Van Durme F, Muller O, Casselman F, De Wiest B, Croes R, Verstreken S, Goethals M, de Raedt H, Sarma J, Joseph L, Vanderheyden M, Weinberg EO. Nonmyocardial production of ST2 protein in human hypertrophy and failure is related to diastolic load. *J Am Coll Cardiol*. 2008;52:2166–2174.
18. Mildner M, Storka A, Lichtenauer M, Mlitz V, Ghannadan M, Hoetzenecker K, Nickl S, Dome B, Tschachler E, Ankersmit HJ. Primary sources and immunological prerequisites for sST2 secretion in humans. *Cardiovasc Res*. 2010;87:769–777.
19. Weinberg EO, Shimpo M, Hurwitz S, Tominaga S, Rouleau JL, Lee RT. Identification of serum soluble ST2 receptor as a novel heart failure biomarker. *Circulation*. 2003;107:721–726.
20. Weir RA, Miller AM, Murphy GE, Clements S, Steedman T, Connell JM, McInnes IB, Dargie HJ, McMurray JJ. Serum soluble ST2: a potential novel mediator in left ventricular and infarct remodeling after acute myocardial infarction. *J Am Coll Cardiol*. 2010;55:243–250.
21. Shimpo M, Morrow DA, Weinberg EO, Sabatine MS, Murphy SA, Antman EM, Lee RT. Serum levels of the interleukin-1 receptor family member ST2 predict mortality and clinical outcome in acute myocardial infarction. *Circulation*. 2004;109:2186–2190.
22. Pascual-Figal DA, Ordoñez-Llanos J, Tornel PL, Vázquez R, Puig T, Valdés M, Cinca J, de Luna AB, Bayes-Genis A; MUSIC Investigators. Soluble ST2 for predicting sudden cardiac death in patients with chronic heart failure and left ventricular systolic dysfunction. *J Am Coll Cardiol*. 2009;54:2174–2179.
23. Barcelos LS, Duplaa C, Kränkel N, et al. Human CD133+ progenitor cells promote the healing of diabetic ischemic ulcers by paracrine stimulation of angiogenesis and activation of Wnt signaling. *Circ Res*. 2009;104:1095–1102.
24. Lee KF, Li E, Huber LJ, Landis SC, Sharpe AH, Chao MV, Jaenisch R. Targeted mutation of the gene encoding the low affinity NGF receptor p75 leads to deficits in the peripheral sensory nervous system. *Cell*. 1992;69:737–749.
25. Emanueli C, Salis MB, Pinna A, Stacca T, Milia AF, Spano A, Chao J, Chao L, Sciola L, Madeddu P. Prevention of diabetes-induced microangiopathy by human tissue kallikrein gene transfer. *Circulation*. 2002;106:993–999.
26. Emanueli C, Minasi A, Zacheo A, Chao J, Chao L, Salis MB, Straino S, Tozzi MG, Smith R, Gaspa L, Bianchini G, Stillo F, Capogrossi MC, Madeddu P. Local delivery of human tissue kallikrein gene accelerates spontaneous angiogenesis in mouse model of hindlimb ischemia. *Circulation*. 2001;103:125–132.
27. Ky B, French B, McCloskey K, et al. High-sensitivity ST2 for prediction of adverse outcomes in chronic heart failure. *Circ Heart Fail*. 2011;4:180–187.
28. Karasek MA. Mechanisms of angiogenesis in normal and diseased skin. *Int J Dermatol*. 1991;30:831–836.
29. Fadini GP, Albiero M, Menegazzo L, Boscaro E, Pagnin E, Iori E, Cosma C, Lapolla A, Pengo V, Stendardo M, Agostini C, Pelicci PG, Giorgio M, Avogaro A. The redox enzyme p66Shc contributes to diabetes and ischemia-induced delay in cutaneous wound healing. *Diabetes*. 2010;59:2306–2314.
30. Nogales-Cadenas R, Carmona-Saez P, Vazquez M, Vicente C, Yang X, Tirado F, Carazo JM, Pascual-Montano A. GeneCodis: interpreting gene lists through enrichment analysis and integration of diverse biological information. *Nucleic Acids Res*. 2009;37(Web Server issue):W317–W322.
31. Siqueira MF, Li J, Chehab L, Desta T, Chino T, Krothpali N, Behl Y, Alikhani M, Yang J, Braasch C, Graves DT. Impaired wound healing in mouse models of diabetes is mediated by TNF-alpha dysregulation and associated with enhanced activation of forkhead box O1 (FOXO1). *Diabetologia*. 2010;53:378–388.
32. Kumar S, Tzimas MN, Griswold DE, Young PR. Expression of ST2, an interleukin-1 receptor homologue, is induced by proinflammatory stimuli. *Biochem Biophys Res Commun*. 1997;235:474–478.
33. Choi S, Friedman WJ. Inflammatory cytokines IL-1β and TNF-α regulate p75NTR expression in CNS neurons and astrocytes by distinct cell-type-specific signalling mechanisms. *ASN Neuro*. 2009;1:.
34. Kumar S, Minnich MD, Young PR. ST2/T1 protein functionally binds to two secreted proteins from Balb/c 3T3 and human umbilical vein endothelial cells but does not bind interleukin 1. *J Biol Chem*. 1995;270:27905–27913.

35. Caporali A, Emanueli C. Cardiovascular actions of neurotrophins. *Physiol Rev*. 2009;89:279–308.
36. Lau E, Ronai ZA. ATF2 - at the crossroad of nuclear and cytosolic functions. *J Cell Sci*. 2012;125:2815–2824.
37. Küchler AM, Pollheimer J, Balogh J, Sponheim J, Manley L, Sorensen DR, De Angelis PM, Scott H, Haraldsen G. Nuclear interleukin-33 is generally expressed in resting endothelium but rapidly lost upon angiogenic or proinflammatory activation. *Am J Pathol*. 2008;173:1229–1242.
38. Findley CM, Mitchell RG, Duscha BD, Annex BH, Kontos CD. Plasma levels of soluble Tie2 and vascular endothelial growth factor distinguish critical limb ischemia from intermittent claudication in patients with peripheral arterial disease. *J Am Coll Cardiol*. 2008;52:387–393.
39. Smadja DM, d'Audigier C, Bièche I, et al. Thrombospondin-1 is a plasmatic marker of peripheral arterial disease that modulates endothelial progenitor cell angiogenic properties. *Arterioscler Thromb Vasc Biol*. 2011;31:551–559.
40. Nakamura T, Funayama H, Kubo N, Yasu T, Kawakami M, Momomura S, Ishikawa SE. Elevation of plasma placental growth factor in the patients with ischemic cardiomyopathy. *Int J Cardiol*. 2009;131:186–191.
41. Becerra A, Warke RV, de Bosch N, Rothman AL, Bosch I. Elevated levels of soluble ST2 protein in dengue virus infected patients. *Cytokine*. 2008;41:114–120.
42. Goldberg MT, Han YP, Yan C, Shaw MC, Garner WL. TNF-alpha suppresses alpha-smooth muscle actin expression in human dermal fibroblasts: an implication for abnormal wound healing. *J Invest Dermatol*. 2007;127:2645–2655.
43. Surapisitchat J, Hoefen RJ, Pi X, Yoshizumi M, Yan C, Berk BC. Fluid shear stress inhibits TNF-alpha activation of JNK but not ERK1/2 or p38 in human umbilical vein endothelial cells: Inhibitory crosstalk among MAPK family members. *Proc Natl Acad Sci USA*. 2001;98:6476–6481.
44. Zhao J, Chen Q, Li H, Myerburg M, Spannhake EW, Natarajan V, Zhao Y. Lysophosphatidic acid increases soluble ST2 expression in mouse lung and human bronchial epithelial cells. *Cell Signal*. 2012;24:77–85.
45. van Dam H, Wilhelm D, Herr I, Steffen A, Herrlich P, Angel P. ATF-2 is preferentially activated by stress-activated protein kinases to mediate c-jun induction in response to genotoxic agents. *EMBO J*. 1995;14:1798–1811.
46. Weinberg EO, Shimpo M, De Keulenaer GW, MacGillivray C, Tominaga S, Solomon SD, Rouleau JL, Lee RT. Expression and regulation of ST2, an interleukin-1 receptor family member, in cardiomyocytes and myocardial infarction. *Circulation*. 2002;106:2961–2966.
47. Matsuyama Y, Okazaki H, Tamemoto H, Kimura H, Kamata Y, Nagatani K, Nagashima T, Hayakawa M, Iwamoto M, Yoshio T, Tominaga S, Minota S. Increased levels of interleukin 33 in sera and synovial fluid from patients with active rheumatoid arthritis. *J Rheumatol*. 2010;37:18–25.

Supplemental Material

Human Patients – Ethical issues

Human studies complied with the ethical principles stated in the "*Declaration of Helsinki*". Human specimens were obtained from patients participating to two studies conducted under the approval of the Ethical Committee of the IRCCS Multimedica, Milan, Italy (IRCCS-Multimedica number: I) 11/2009 and II) 020/2008). In addition, NHS NRES 11SW/0093 approval was obtained for human sample import, storage, and analysis at the University of Bristol, Bristol, UK. Both are pilot observational studies with the objective of defining cellular and molecular targets of diabetic CLI by analyzing tissue samples from surgical leftovers and peripheral blood samples. The access to this sample collection allowed us to conduct a retrospective analysis of parameters of interest.

Briefly, study I) 11/2009 was designed to dissect the effect of diabetes on the expression of molecular targets to design new targeted therapies for the cure of ischemic diabetic ulcers in patients with chronic limb ischemia (CLI). After obtainment of informed written consent, a consecutive series of patients was recruited. Two groups were studied: 1) non-diabetic and non-ischemic patients undergoing vena saphena stripping (controls, n=10); 2) diabetic patients with CLI undergoing major limb amputation (n=14). This study provided limb amputation samples for IHC and peripheral blood for serum analysis.

Study II) 020/2008 aims to determine the mechanisms responsible for vascular progenitor cell dysfunction in the perspective of new therapies for the cure of the diabetic foot (ClinicalTrials.gov: NCT01269580, Title: Diabetic Foot and Vascular Progenitor Cells). Events analyzed at the follow up time, 12 month after percutaneous angioplasty (PTA) procedure was performed, are: cardiovascular mortality for all causes, major amputation, and post-angioplasty restenosis in treated limb. Two groups of patients with CLI undergoing PTA procedure were analyzed: 2) non-diabetic patients with CLI (n=8); 3) diabetics patients with CLI (n=53). This study provided peripheral blood samples for serum analysis and follow up data for clinical-laboratory data correlation. CLI was defined according to TASC criteria (2007): pain at rest, and/or ulcer or gangrene due to artheropaty: transcutaneous oximetry < 30 mmHg or pressure on the ankle < 70 mmHg. Exclusion criteria were drug-induced diabetes, liver failure or dialysis due to renal failure, cancer with adverse prognosis in months, or chemotherapic treatment, pregnancy, lack of consent to participate to the study.

Animal procedures

All procedures complied with the standards stated in the *Guide for the Care and Use of Laboratory Animals* (Institute of Laboratory Animal Resources, National Academy of

Sciences, Bethesda, MD, USA, 1996) and approved by the UK Home Office. C57BL/6J-*p75*$^{NTR-/-}$ (*p75KO*) [1] and *p75*$^{NTR+/+}$ (*WT*) littermates were bred at the University of Bristol starting from breeding pairs kindly provided by Prof. Beth Habecker, Oregon Health and Science University. Seven to eight weeks old male *p75KO* and *WT* mice were made diabetic using streptozotocin (Sigma) (STZ, 40 mg/kg in 0.1mol/l citrate buffer pH4.5 i.p. per day for 5 days)[2] or left normoglycemic by STZ buffer injections. For the STZ groups, persistence of glycosuria ≥10 g/L was checked over the duration of the experiments. One or three months after diabetes induction, anesthetized (Avertin, 880 mmol/kg, i.p., Sigma) mice underwent induction of unilateral hindlimb ischemia by permanent ligation and electro-coagulation of the proximal end of left femoral arteries. At the same time, a full thickness wound was created in the thigh dorsal skin of the ischemic legs using a sterile 5-mm-wide biopsy punch[3]. After surgery, animals were maintained in cages with food and water *ad libitum* and in a temperature and humidity-controlled environment. Laser Doppler perfusion image analysis (Perimed) was performed at baseline to confirm limb ischemia and at 3, 7 and 14 days thereafter to monitor BF recovery[4]. Clinical outcome was established by determining the rate of wound closure[3]. To this aim, two perpendicular diameters of the wound were measured by using a Vernier caliper and wound area was calculated using a standard formula for the area of an ellipse (semi-major diameter X semi-minor diameter X Pi). Wound area was evaluated immediately after punching and then at 3, 7 and 14 days afterwards. Mice were sacrificed at either 3 or 14 days post-surgery. At 3 days, mice were sacrificed by an overdose of anaesthetic and the wounds and surrounding skin were removed and perpendicularly cut into two halves. One half was immediately frozen for molecular biology studies while the other was fixed in 4% buffered formalin solution and further processed for histology or immunohistochemical analyses. At 14d post-surgery, the limbs of terminally anaesthetised mice were perfusion/fixed and ischaemic adductor muscles harvested and processed for paraffin embedding.

RNA extraction, microarray and quantitative RT-PCR on mouse samples

RNA was extracted from wounds using the FastPrep tissue lyser (MPbio) and RNeasy AllPrep kits (Qiagen). Twelve single channel hybridisations (using Cy3-dye) on Agilent 4x44k arrays were analysed. Gene ontology (GO analysis) enrichment analysis was carried out using GeneCodis 2.0[5] (www.http://genecodis.dacya.ucm.es). Array data were registered in GEO (accession number: GSE34675). Quantitative RT-PCR (Q-PCR) *sfrp1* (Secreted frizzled-related protein 1), *Hpx* (Hemopexin), *clu* (Clusterin), *tnc* (Tenascin), *krt20* (Keratin 20), *vegfa* (vascular endothelial growth factor A), *vezf1* (vascular endothelial zinc finger 1), *itgb1* (integrin beta-1), *birc5* (survivin), *pttg1* (securin) and *il-33* and for the housekeeping *hprt1*(hypoxanthine phosphoribosyltransferase 1) and *rpl13a* (60S ribosomal protein L13a)

or *18s* (18s ribosomal RNA) was performed using validated primers (Applied Biosystems). For murine *il1rl1* (*ST2*, sequence shared by both isoforms) primer sequences are: sST2 forward 5'-CTTGTTCTCCCCGCAGTC-3', reverse 5'- CCAATGTCCCTTGTAGTCGG-3' probe 5'-TCCCCATCTCCTCACCTCCCTTAAT 3'; mouse ST2L forward 5'-TCTGTGGAGTACTTTCACC-3' reverse 5'-TCTGCTATTCTGGATACTGCTTTC-3' probe 5'-AGAGACCTGTTACCTGGGCAAGATG-3'. Data normalisation was performed by geometric averaging.[6]

Immunhistochemistry on human and murine tissues

Sections of tissue (5 μm) were deparaffinized in xylene and rehydrated. Slides were incubated in a solution of 0.5% hydrogen peroxidase in methanol followed by antigen retrieval in 0.5 M citrate buffer (pH 6) and incubation in 2.5% horse serum (Vector Laboratories). Sections were stained overnight with rabbit anti-mouse ST2 (Abnova), rabbit anti-human ST2 (Sigma), rabbit anti-mouse $p75^{NTR}$ (Abcam), rat anti-mouse CD31 (BD Biosciences) or appropriate IgG control (Dako), followed by incubation with ImmPRESS reagent horse anti-mouse Ig or anti-rabbit Ig (Vector Laboratories). Signal was developed using the peroxidase substrate DAB (Vector Laboratories). Harris's haematoxylin (BDH) was used for counterstaining. For fluorescent immunohistochemistry, secondary antibodies were goat anti-rabbit or goat anti-mouse conjugated to Alexa-488 or Alexa-568 fluorophores (Molecular Probes).

Microvascular density in wounds was counted after staining for CD31. Apoptosis of ECs was assessed by in situ TUNEL assay combined with CD31 staining. Muscular capillary and arteriole densities were measured in transverse section (5μm thickness) of the ischemic adductor and gastrocnemius muscles after staining with fluorescent isolectin-B4 (EC marker; 1:100, Invitrogen) and with an antibody for α-smooth muscle actin (α-SMA, 1:400, for marking vascular smooth muscle cells, Sigma). Fifteen fields (20X magnification) were randomly examined and averaged to analyze number of capillaries, while number of small arterioles (diameter ≤ 50μm) were analysed considering whole muscle area. Capillary and arteriole density is expressed per square millimetre.

Statistical Analyses

Group differences of continuous variables were compared by one-way ANOVA or Student *t* test, as appropriate. Continuous data are expressed as mean ± SEM. A *P* value <0.05 was considered statistically significant.

For statistical analysis of microarray experiments, all exploratory data analysis and all data pre-processing were performed in R / Bioconductor. Data preprocessing included the

following steps: background correction using Agilent spatial detrending background estimate, averaging of replicate spots, log2-transformation, KNN imputation of missing values, unsupervised filtering (IQR threshold) to get rid of uninformative probes (low variance), Quantile Normalisation. For inference statistics, the linear modelling functions provided by the Limma package were used. Determinants of the prognostic value of circulating sST2 levels were assessed using multivariate linear regression methods, with the natural log-transformed form of sST2 as the dependent variable. The effect of each determinant was derived from exponentiated regression coefficients [7]. Statistical analyses on patients were completed using R 2.13.3, including the MASS library.

References for the Online Methods

1. Lee KF, Li E, Huber LJ, Landis SC, Sharpe AH, Chao MV, Jaenisch R. Targeted mutation of the gene encoding the low affinity ngf receptor p75 leads to deficits in the peripheral sensory nervous system. *Cell*. 1992;69:737-749
2. Emanueli C, Salis MB, Pinna A, Stacca T, Milia AF, Spano A, Chao J, Chao L, Sciola L, Madeddu P. Prevention of diabetes-induced microangiopathy by human tissue kallikrein gene transfer. *Circulation*. 2002;106:993-999
3. Barcelos LS, Duplaa C, Krankel N, Graiani G, Invernici G, Katare R, Siragusa M, Meloni M, Campesi I, Monica M, Simm A, Campagnolo P, Mangialardi G, Stevanato L, Alessandri G, Emanueli C, Madeddu P. Human cd133+ progenitor cells promote the healing of diabetic ischemic ulcers by paracrine stimulation of angiogenesis and activation of wnt signaling. *Circ Res*. 2009;104:1095-1102
4. Caporali A, Pani E, Horrevoets AJ, Kraenkel N, Oikawa A, Sala-Newby GB, Meloni M, Cristofaro B, Graiani G, Leroyer AS, Boulanger CM, Spinetti G, Yoon SO, Madeddu P, Emanueli C. Neurotrophin p75 receptor (p75ntr) promotes endothelial cell apoptosis and inhibits angiogenesis: Implications for diabetes-induced impaired neovascularization in ischemic limb muscles. *Circ Res*. 2008;103:e15-26
5. Nogales-Cadenas R, Carmona-Saez P, Vazquez M, Vicente C, Yang X, Tirado F, Carazo JM, Pascual-Montano A. Genecodis: Interpreting gene lists through enrichment analysis and integration of diverse biological information. *Nucleic Acids Res*. 2009;37:W317-322
6. Vandesompele J, De Preter K, Pattyn F, Poppe B, Van Roy N, De Paepe A, Speleman F. Accurate normalization of real-time quantitative rt-pcr data by geometric averaging of multiple internal control genes. *Genome Biol*. 2002;3:RESEARCH0034
7. Ky B, French B, McCloskey K, Rame JE, McIntosh E, Shahi P, Dries DL, Tang WH, Wu AH, Fang JC, Boxer R, Sweitzer NK, Levy WC, Goldberg LR, Jessup M, Cappola TP. High-sensitivity st2 for prediction of adverse outcomes in chronic heart failure. *Circ Heart Fail*. 2011;4:180-187

Supplementary Table I: Clinical outcome at one-year follow up for the 53 diabetic patients undergoing revascularization for critical limb ischemia

Patients	Diabetics with CLI undergoing Revascularization (n=53)
Restenosis	29/53 RES
Amputation	7/53 AMP
Death	6/53 D

AMP=amputation, RES=restenosis, D=death

Supplementary Table II: List of 40 genes which are differentially expressed in the ischemic wounds of diabetic wild type (WT) mice vs, non-diabetic WT mice and whose expression in diabetes was normalised by *p75^{NTR}* gene knock-out (p75KO).

Gene Symbol	Gene name	logFC WT no diab vs WT diab	logFC WT diab vs p75KO diab
Lhx8	LIM homeobox protein 8	-3.987	-3.828
Hpx	Hemopexin	-1.122	-1.861
Krt20	keratin 20	-0.656	-1.598
Trh	thyrotropin releasing hormone	-1.248	-1.340
Pnet-ps	prenatal ethanol induced mRNA, pseudogene	-1.008	-1.292
Clu	Clusterin	-0.868	-1.195
Syt13	synaptotagmin XIII	-0.886	-1.155
Penk	Preproenkephalin	-1.553	-1.082
Il1rl1	interleukin 1 receptor-like 1	-1.468	-1.074
Fam148b	family with sequence similarity 148, member B	-0.913	-1.065
Tmem56	transmembrane protein 56	-0.611	-1.018
Cbln1	cerebellin 1 precursor protein	-1.355	-0.899
Pot1b	protection of telomeres 1B	-0.812	-0.894
Abcd3	ATP-binding cassette, sub-family D (ALD), 3	-1.147	-0.845
Pogz	pogo transposable element with ZNF domain	-0.964	-0.799
Stc1	stanniocalcin 1	-1.039	-0.798
Tnc	tenascin C	-1.375	-0.790
Olfr351	olfactory receptor 351	-0.924	-0.727
Fam167a	family with sequence similarity 167, member A	-0.701	-0.701
Mc5r	melanocortin 5 receptor	-0.776	-0.699
Igk-V38	immunoglobulin kappa chain	-0.793	-0.670

	variable 38(V38)		
Fam55c	family with sequence similarity 55, member C	-0.950	-0.604
Tinagl1	tubulointerstitial nephritis antigen-like 1	-0.684	-0.581
Oosp1	oocyte secreted protein 1	0.531	0.595
Olfr836	olfactory receptor 836	0.847	0.614
Ropn1l	ropporin 1-like	0.581	0.681
D1Pas1	DNA segment, Chr 1, Pasteur Institute 1	1.073	0.735
Frem2	Fras1 related extracellular matrix protein 2	0.665	0.752
Tmie	transmembrane inner ear	0.671	0.756
Hormad1	HORMA domain containing 1	0.651	0.784
Gm2824	predicted gene 2824	0.656	0.805
Gm5087	predicted gene 5087	0.979	0.819
Serpina1f	serine (or cysteine) peptidase inhibitor, 1F	0.855	0.871
Dpys	Dihydropyrimidinase	0.902	0.914
Prkce	protein kinase C, epsilon	0.892	0.920
Creg2	cellular repressor of E1A-stimulated genes 2	0.714	0.929
Ly9	lymphocyte antigen 9	0.924	1.106
Usp11	ubiquitin specific peptidase 11	1.710	1.204
F7	coagulation factor VII	1.410	1.539
Arl5c	ADP-ribosylation factor-like 5C	0.742	1.569

LogFC: log fold change.

<u>Supplementary Table III:</u> Correlation between sST2 and other variables in 53 diabetic patients with critical limb ischemia undergoing surgical revascularization

Coefficient	Effect on ST2 (%)	Est. coef. on log(ST2)	Std. Error	t value	Pr(>|t|)
(Intercept)	--	4.671	0.261	17.904	0
Anti-glycemic drugs at baseline	-56.2	-0.5620	0.22	-2.547	0.015
Death by 12 months	59.9	0.599	0.263	2.271	0.028
Platelet count at the baseline	0.1	0.001	0.0007	0.0739	0.941
Anti-platelet agents at baseline	-31.1	-0.3116	0.1832	-1.701	0.097

.

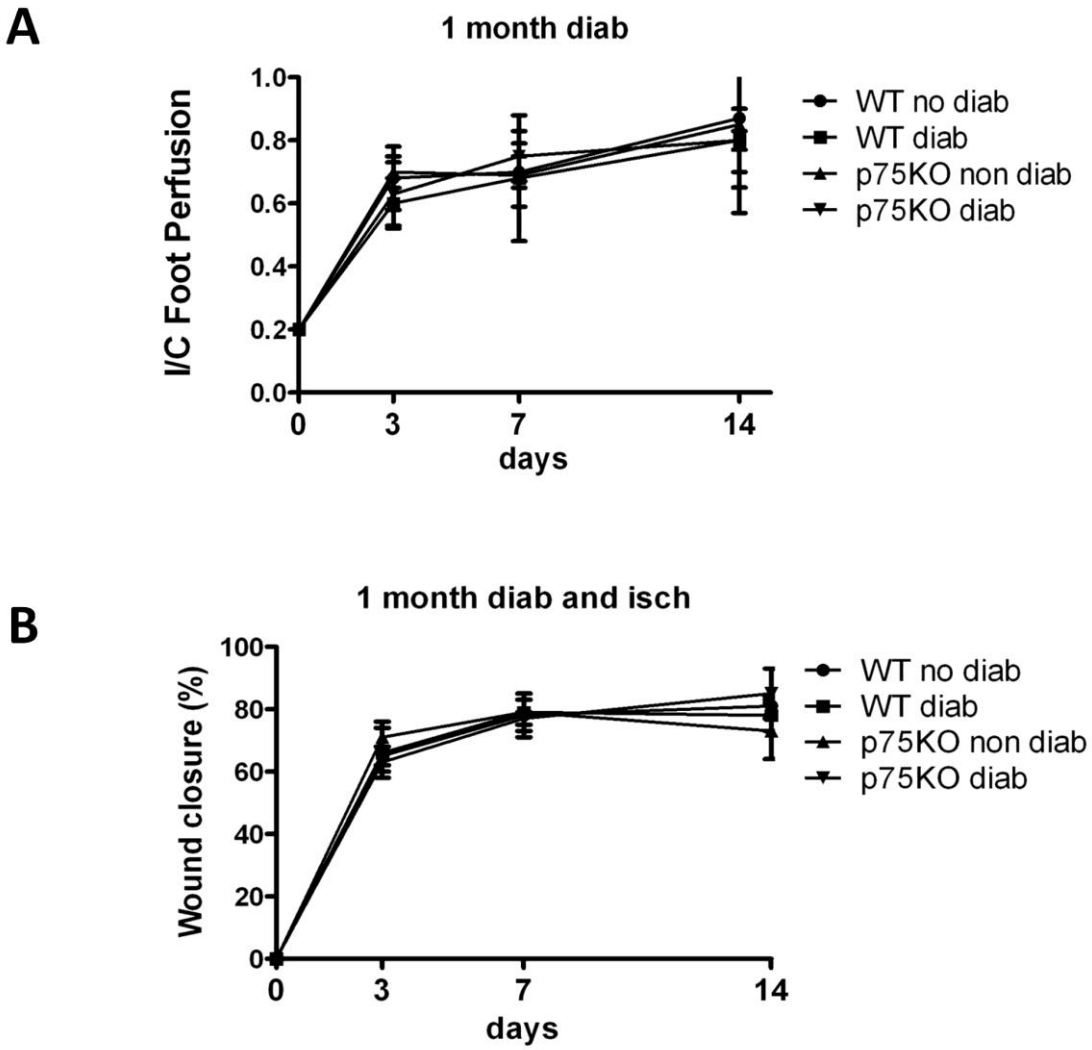

Supplementary Figure I: Blood flow recovery and wound healing in mice with one months of diabetes. A, Unilateral limb ischemia was performed in diabetic (Diab) and non-diabetic (non Diab) wild-type (WT) and $p75^{NTR}$-knockout (p75KO) mice after 1 months of diabetes. Line graph shows the time-course of post-ischemic foot blood flow (BF) recovery (calculated as the ratio between ischaemic and contra-later foot BF). **B**, Healing of a 5-mm–diameter cutaneous wound was monitored using digital photography in WT and p75KO diabetic (Diab) and nondiabetic (Non Diab) mice after 1 month of diabetes with hind limb ischemia. Wound size is reported as percentage of the initial wound area. Data represent means ± SEM.

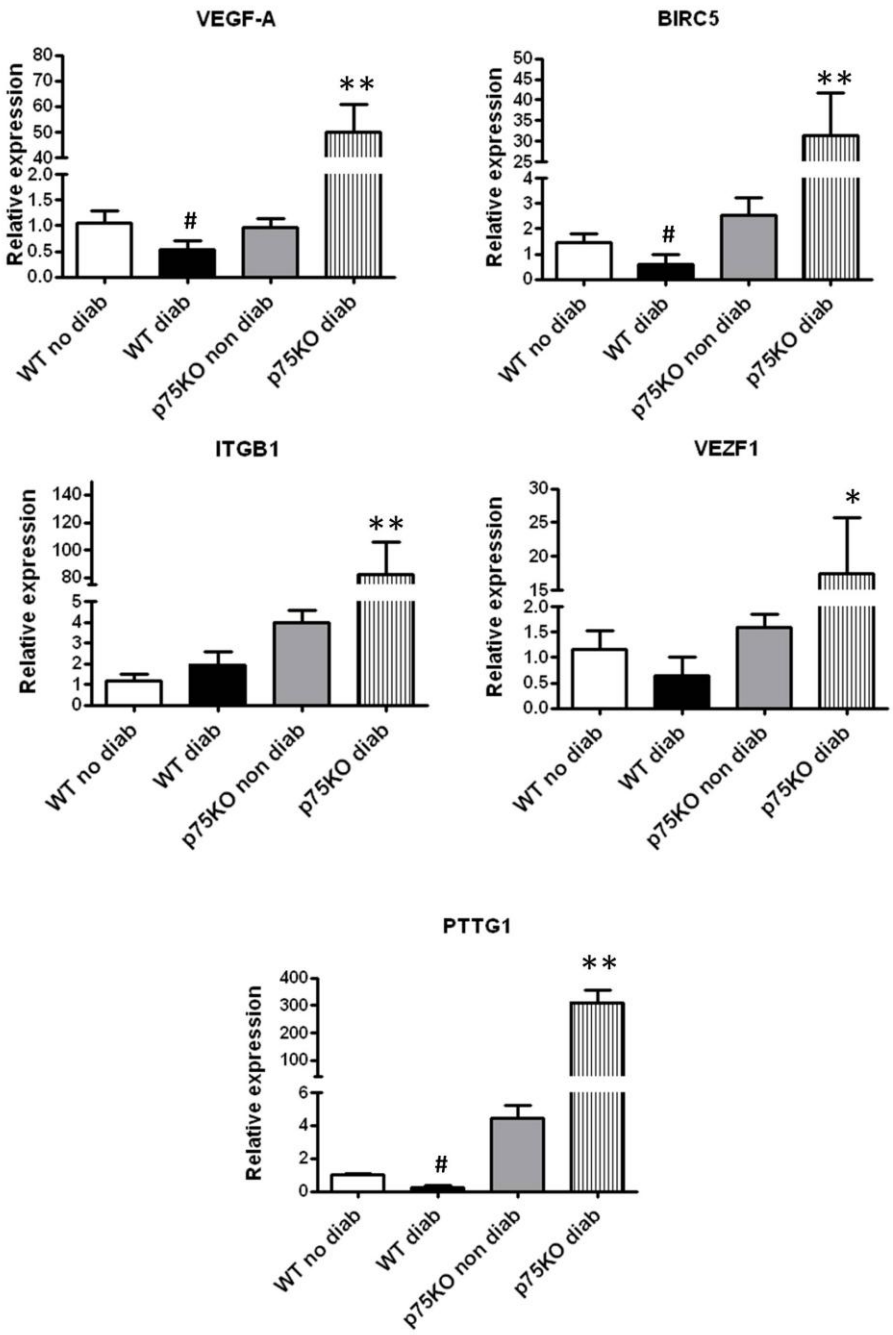

Supplementary Figure II: Modulation of p75^{NTR}-regulated genes in adductor muscles by diabetes in WT and p75KO mice Expression levels of selected genes (*vegfa*, *birc5*, *itgb1*, *vezf1*, *pttg1*) in skin wounds were determined using Q-PCR. Results were normalized to 18S expression. Q-PCR data represent means ± SEM (*n*=5). #p<0.05 vs. non-diabetic *WT* mice; *p<0.05 vs. diabetic *WT* mice.

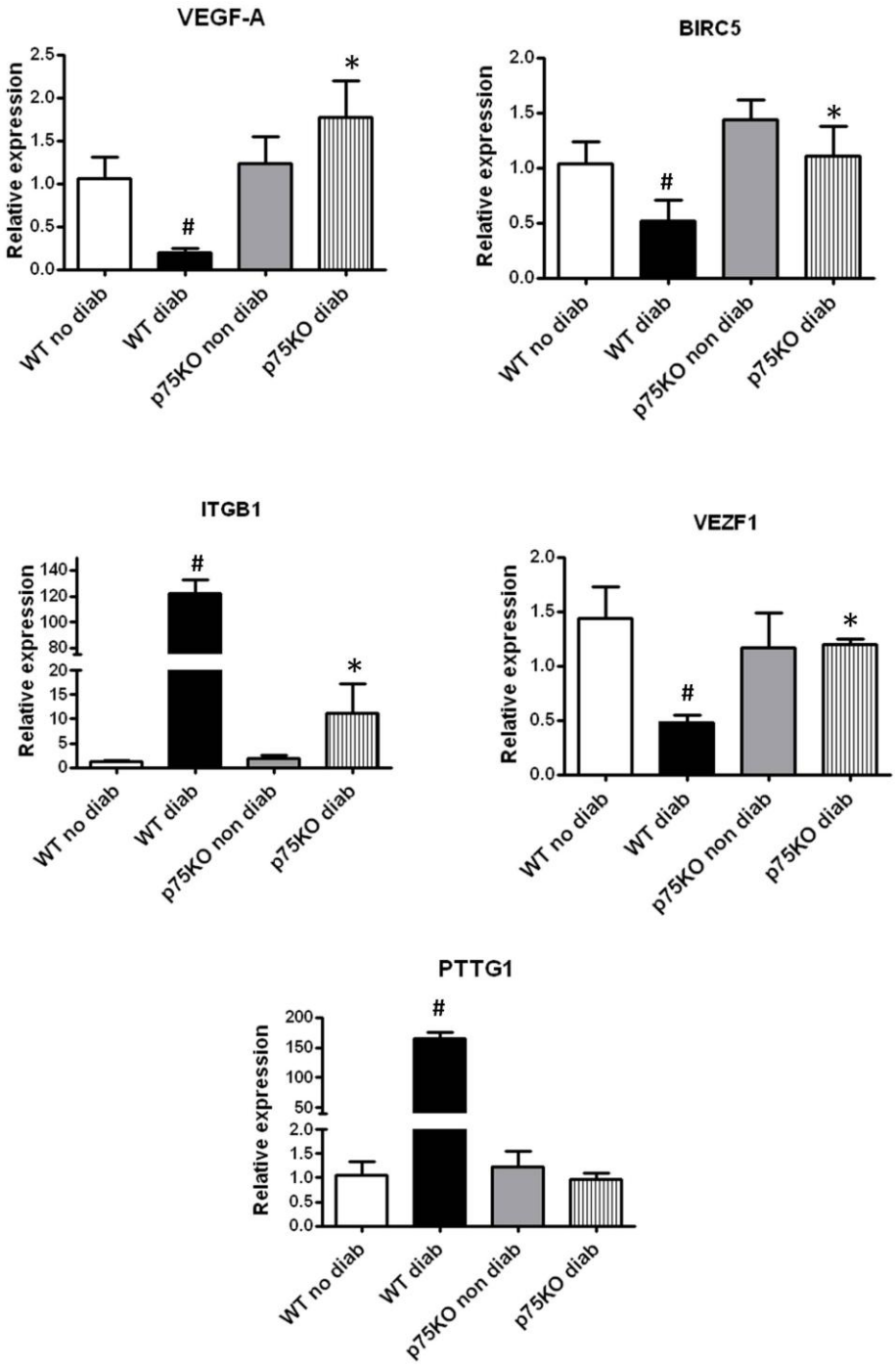

Supplementary Figure III: Modulation of p75^{NTR}-regulated genes in skin wounds by diabetes in WT and p75KO mice . Expression levels of selected genes (*vegfa*, *birc5*, *itgb1*, *vezf1*, *pttg1*) in adductor muscles were determined using Q-PCR. Results were normalized to 18S expression. Q-PCR data represent means ± SEM (*n*=5). #p<0.05 vs. non-diabetic *WT* mice; *p<0.05 vs. diabetic *WT* mice.

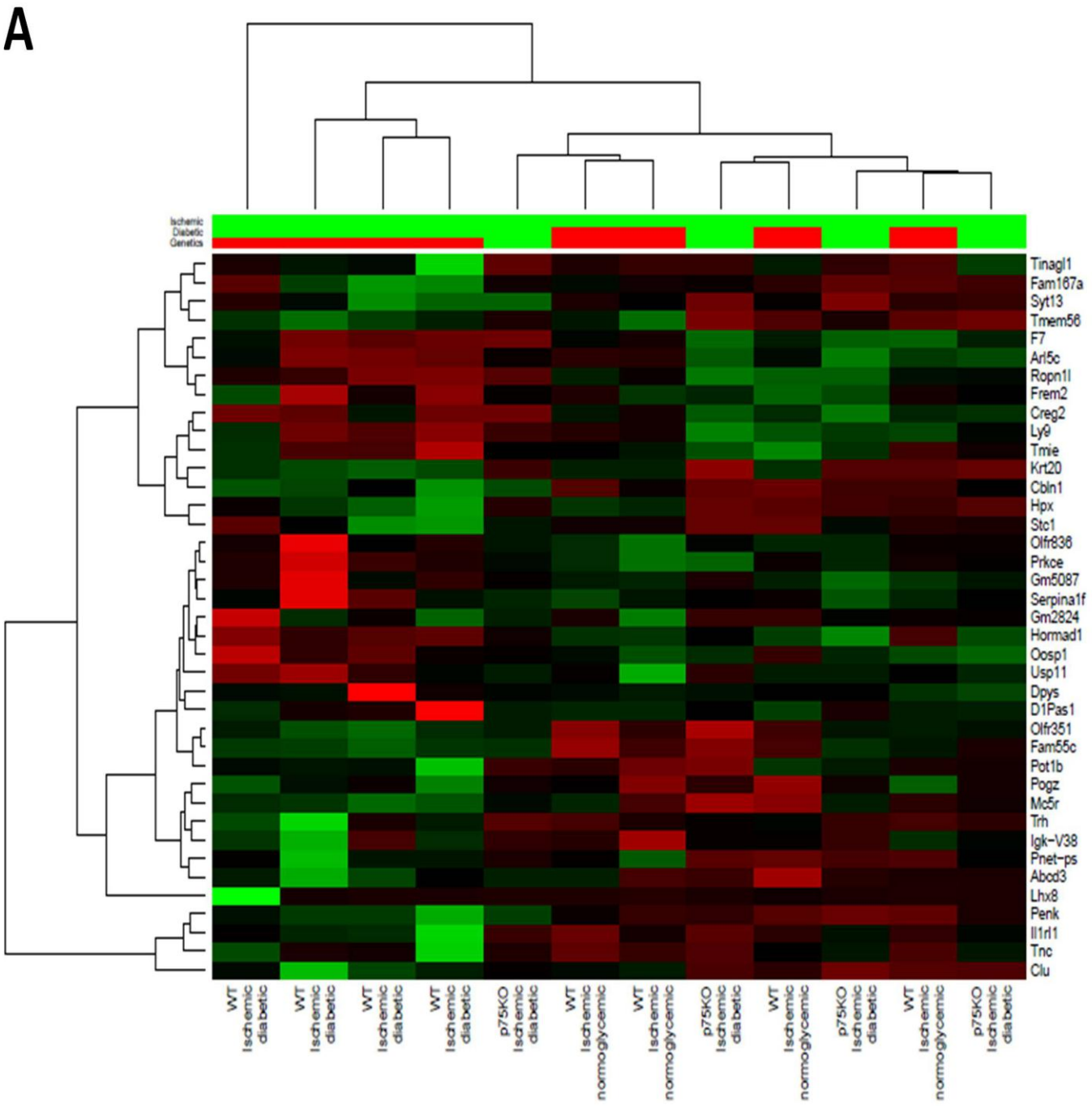

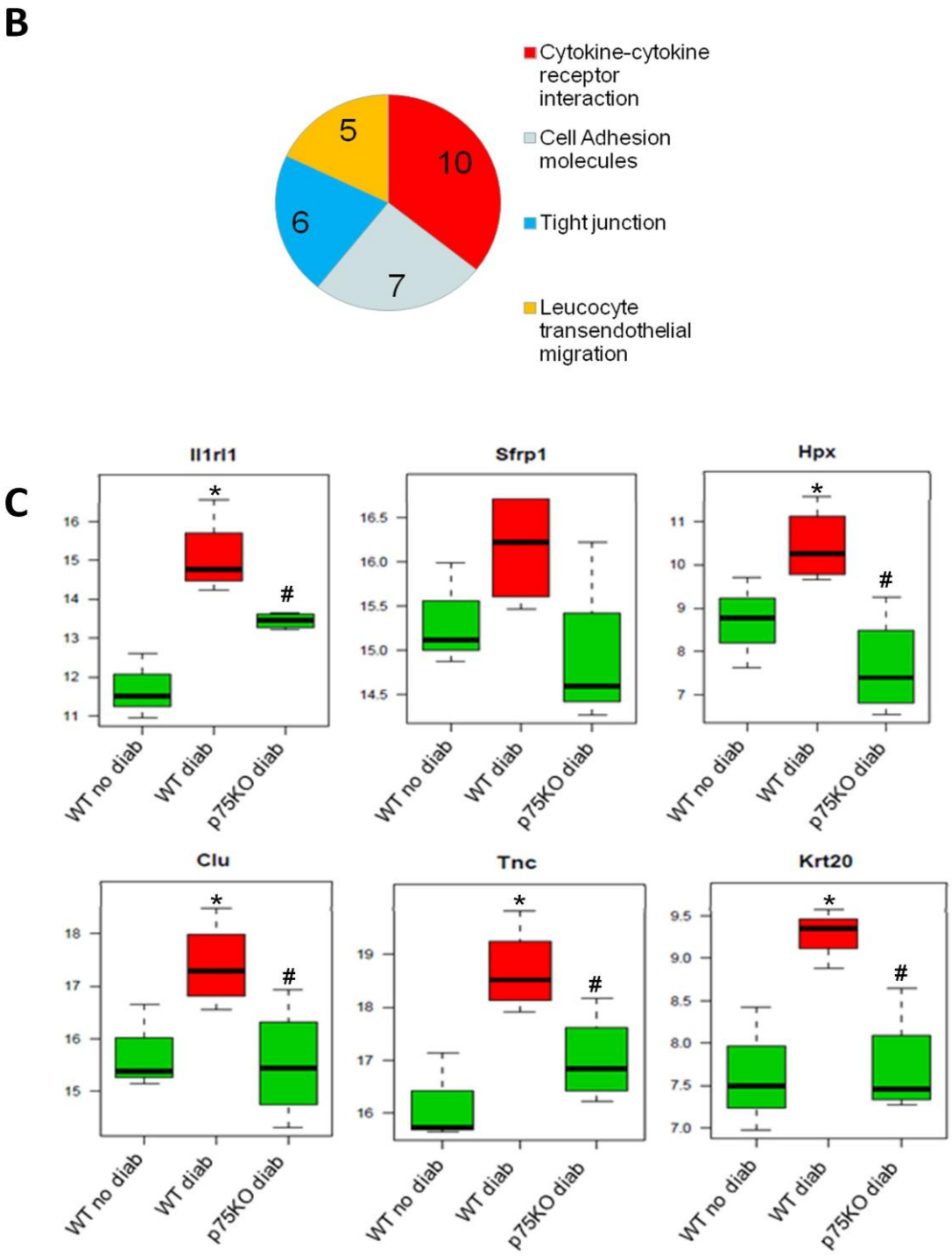

Supplementary Figure IV: Modulation of gene profile in skin wounds by diabetes in WT and p75KO mice. A, Heatmap of differentially expressed genes in the ischemic wounds of diabetic WT mice vs WT non diabetic mice and whose expression was normalized in diabetic p75KO mice. **B,** Gene ontology annotation analysis using Genecodis 2.0. **C,** Validation of microarray expression analysis. Expression levels of selected genes (IL1RL1 (ST2), sFRP1 Hpx, CLU, Tnc, Krt20) were independently determined using Q-PCR. Results were normalized to HPRT and RPL13a expression. Q-PCR data represent means ± SEM (*n*=3). #p<0.05 vs. non-diabetic *WT* mice; *p<0.05 vs.. diabetic WT mice.

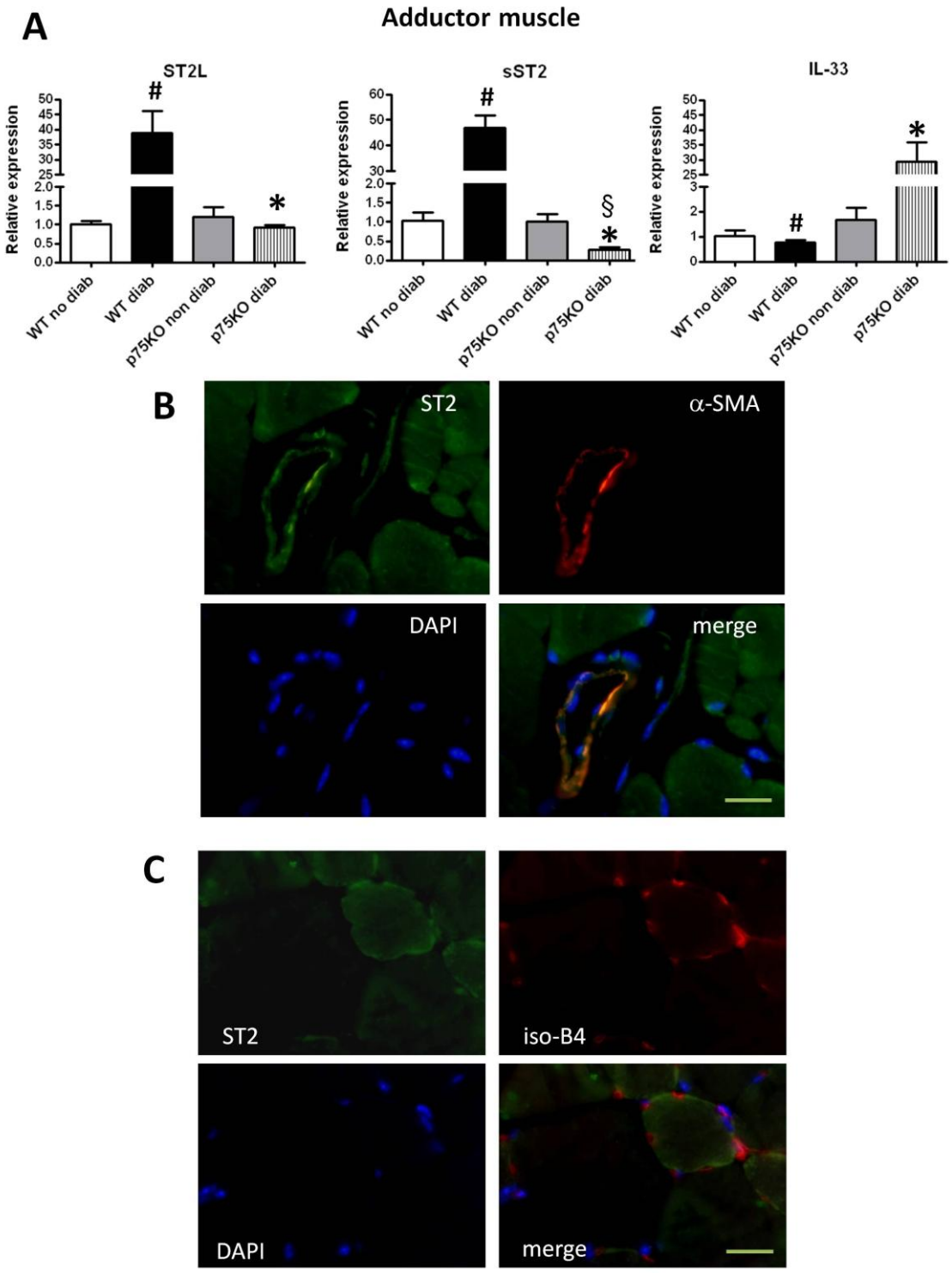

Supplementary Figure V: IL-33 and ST2 expression in adductor muscles. A, Relative mRNA expression of ST2L, sST2 and IL-33 in adductor muscles of diabetic and non-diabetic *WT* and *p75KO* mice**.** Results are normalized to 18S expression. Data represent means ± SEM, *n* = 5 *p<0.05 vs. diabetic *WT* mice; #p<0.05 vs. non-diabetic *WT* mice. §p<0.05 vs non diabetic *p75KO* mice. **B**, Fluorescent immonocytochemistry for ST2 (green fluorescence), and α-SMA(red fluorescence) in ischemic adductor muscles of diabetic *WT* mice. Nuclei were counterstained with DAPI (blue fluorescence). **C**, Fluorescent immonocytochemistry for ST2 (green fluorescence), and isolectin–B4 (red fluorescence) in ischemic adductor muscles of diabetic *WT* mice. Nuclei were counterstained with DAPI (blue fluorescence). Magnfication: 100x. Scale bar, 10μm

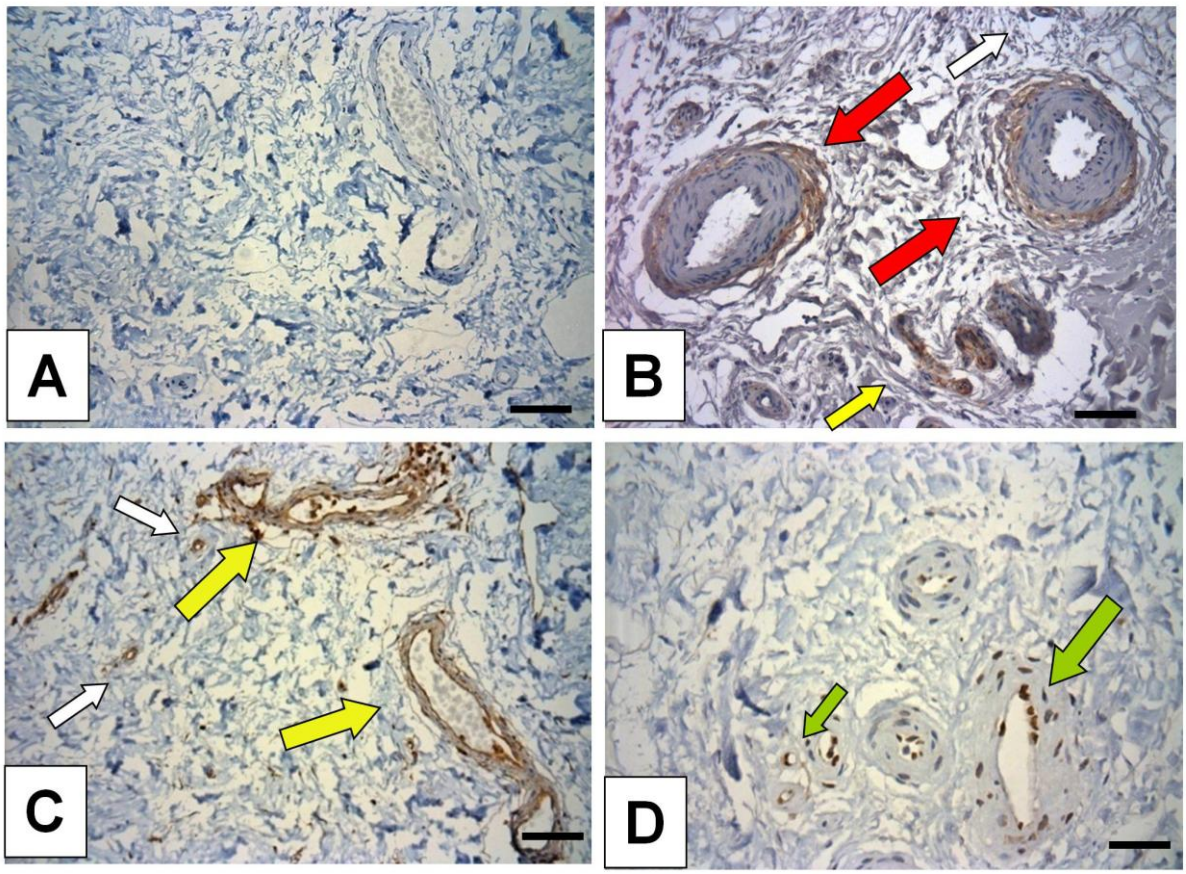

Supplementary Figure VI: Detection and localization of p75^{NTR}, ST2 and IL-33 in the human skin from amputated ischemic legs of diabetic patients. p75^{NTR}, ST2 and IL-33 are expressed in human skin. Human skin biopsies from amputated diabetic patients were paraffin processed and immunostained for isotype control (panel a), p75^{NTR} (panel b), ST2 (panel c) and IL-33 (panel d). Representative histology of *n*=5 patients is shown. Magnification 40×; scale bars: 5 μm. Venules: yellow arrows; Small arteries: red arrows; Microvessels: white arrows; EC Nuclear staining: green arrows.

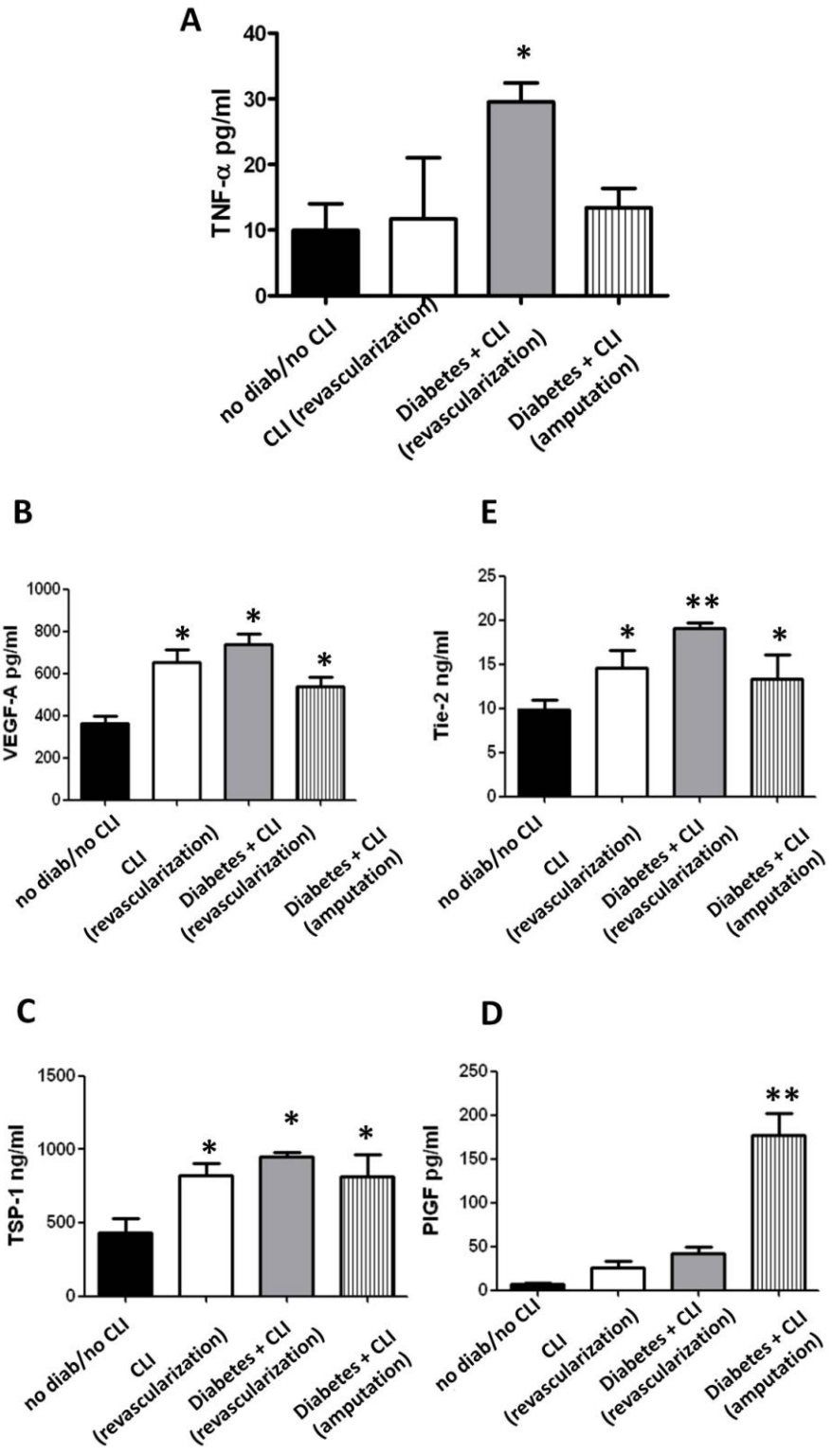

Supplementary Figure VII: Circulating levels of TNF-α, VEGF-A, soluble Tie-2, TSP-1, and PIGF in patients with critical limb ischemia and controls. Serum levels of TNF-α, VEGF-A, soluble Tie-2, TSP-1 and PIGF in non-diabetic non-ischemic controls (n=11), non-diabetic patients critical limb ischemia (CLI) undergoing revascularization (n=8), diabetics patients with CLI undergoing revascularization (n=53), and diabetic patients with CLI undergoing limb amputation. (n=14). ELISA data represent means ± SEM. *p<0.05 vs controls.

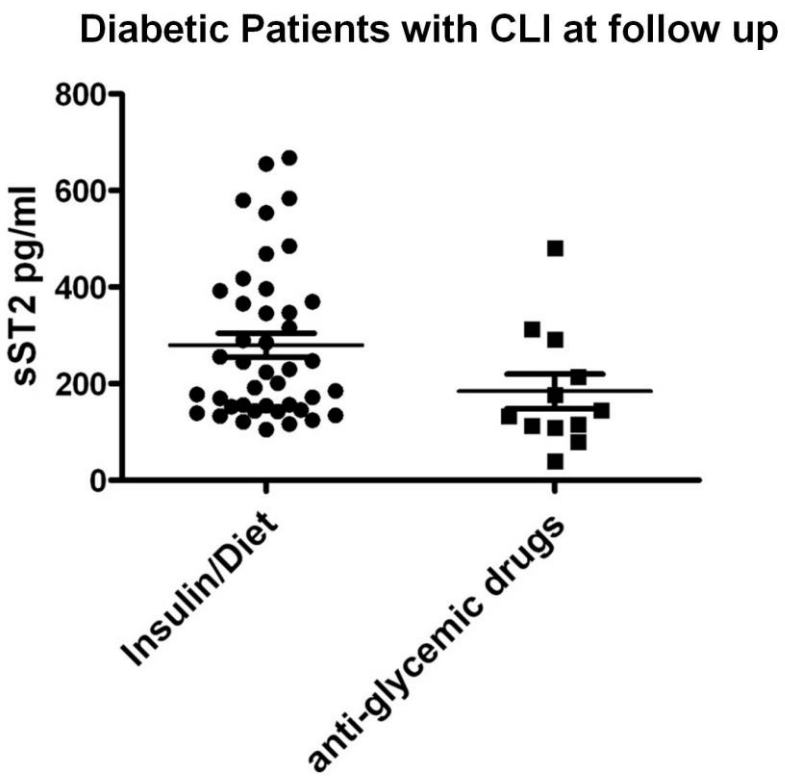

Supplementary Figure VIII: Correlation between sST2 and use of antiglycemic drugs. Dot plot showing the baseline concentrations of sST2 in diabetic patients with CLI undergoing revascularization and treated (black circle) or not (black bars) with anti-glycemic drugs.

Densitometry Western blot Figure 4

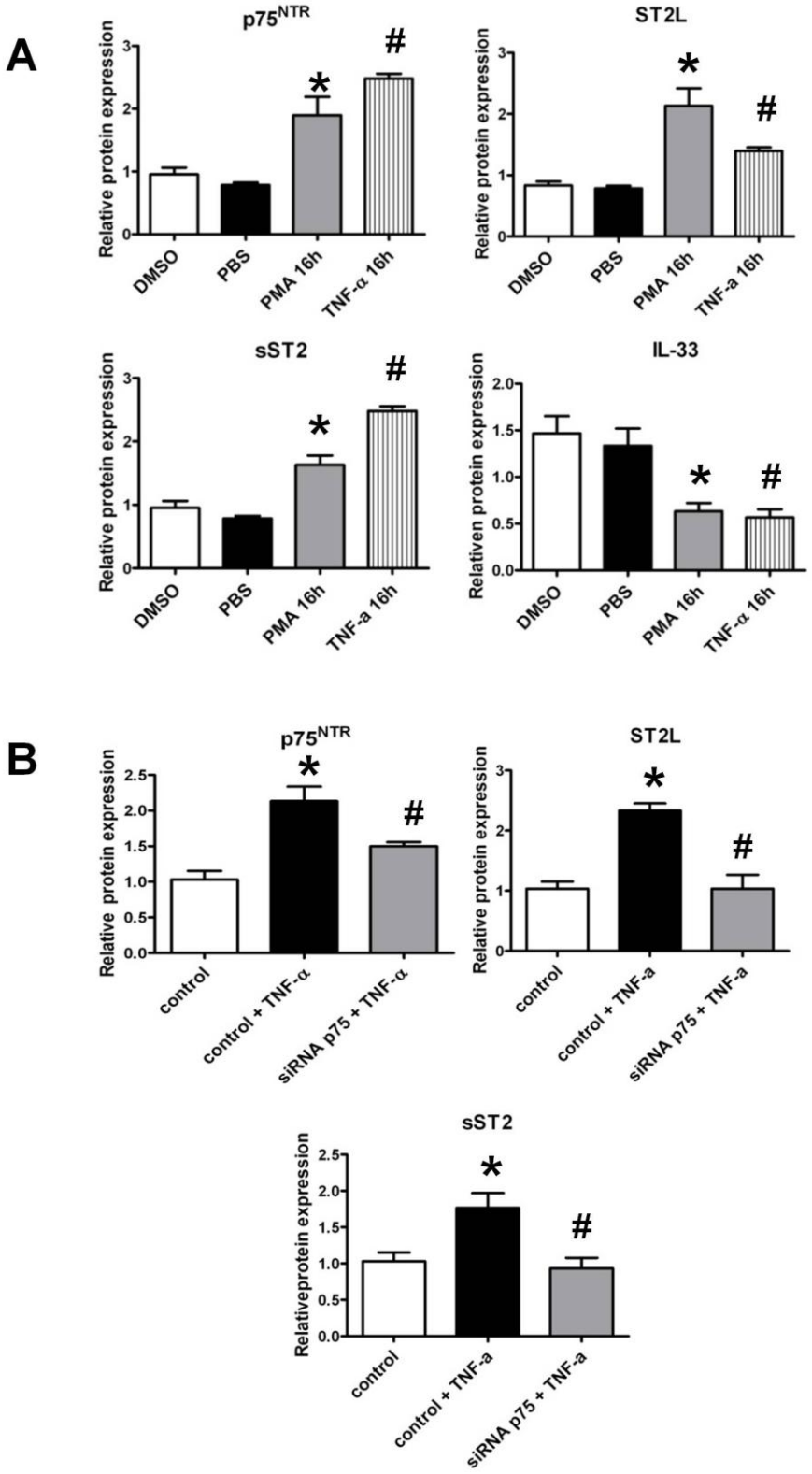

E **Densitometry Western blot Figure 4**

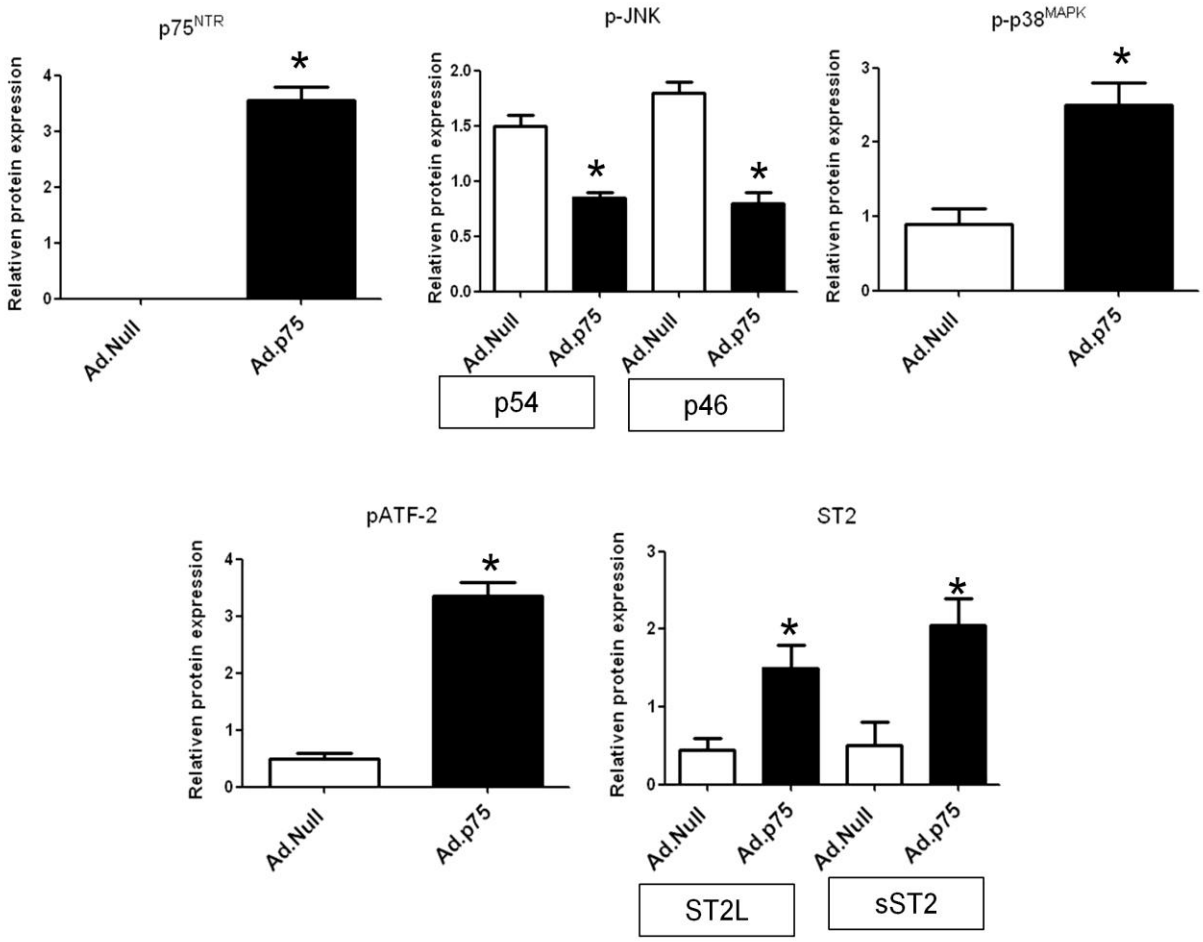

F

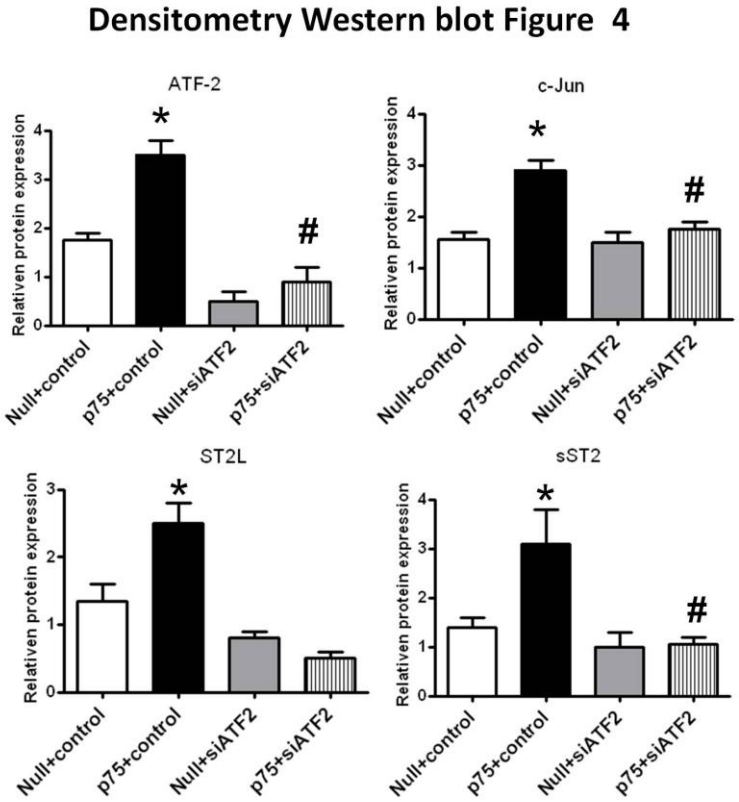

G

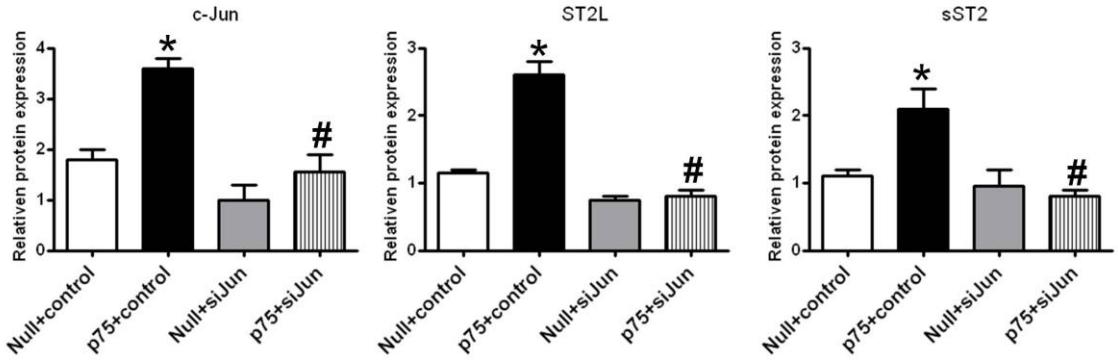

Supplementary Figure IX: Densitometry quantification of western blot analyses shown in Figure 4; A, Bar graphs show relative protein quantification of $p75^{NTR}$, sST2, ST2L and IL-33. Relative values are normalized by α/β Tubulin levels. *p<0.05 vs. DMSO (vehicle PMA); #p<0.05 vs. PBS (vehicle TNF-α). **B,** Bar graphs show relative protein quantification of $p75^{NTR}$, sST2 and ST2L. Relative values are normalized by α/βTubulin levels. *p<0.05 vs. control; #p<0.05 vs control+TNF-α. **E,** Bar graph show relative protein quantification of $p75^{NTR}$, $p\text{-}38^{MAPK}$, p-JNK, p-ATF-2, sST2 and ST2L. Relative values are normalized by α/β Tubulin levels or total protein. *p<0.05 vs. *Ad.Null*; **F,** Bar graph show relative protein quantification of ATF-2, c-Jun, sST2 and ST2L. Relative values are normalized by α/β Tubulin levels. *p<0.05 vs. *Ad.Null*+control; #p<0.05 vs *Ad.p75*+control; **G,** Bar graph show relative protein quantification of c-Jun, sST2 and ST2L. Relative values are normalized by α/β Tubulin levels. *p<0.05 vs. *Ad.Null*+control; #p<0.05 vs. *Ad.p75*+control